

AWARD NUMBER: W81XWH-06-C-0051

TITLE: Mathematical Modeling of Physical and Cognitive Performance Decrement
from Mechanical and Inhalation Insults

PRINCIPAL INVESTIGATOR: James H. Stuhmiller

CONTRACTING ORGANIZATION: L-3 Services, Inc.
San Diego, CA 92121

REPORT DATE: December 2009

TYPE OF REPORT: Annual

PREPARED FOR: U.S. Army Medical Research and Materiel Command
Fort Detrick, Maryland 21702-5012

DISTRIBUTION STATEMENT: Approved for Public Release;
Distribution Unlimited

The views, opinions and/or findings contained in this report are those of the author(s) and should not be construed as an official Department of the Army position, policy or decision unless so designated by other documentation.

REPORT DOCUMENTATION PAGE			<i>Form Approved</i> <i>OMB No. 0704-0188</i>		
Public reporting burden for this collection of information is estimated to average 1 hour per response, including the time for reviewing instructions, searching existing data sources, gathering and maintaining the data needed, and completing and reviewing this collection of information. Send comments regarding this burden estimate or any other aspect of this collection of information, including suggestions for reducing this burden to Department of Defense, Washington Headquarters Services, Directorate for Information Operations and Reports (0704-0188), 1215 Jefferson Davis Highway, Suite 1204, Arlington, VA 22202-4302. Respondents should be aware that notwithstanding any other provision of law, no person shall be subject to any penalty for failing to comply with a collection of information if it does not display a currently valid OMB control number. PLEASE DO NOT RETURN YOUR FORM TO THE ABOVE ADDRESS.					
1. REPORT DATE 1 December 2009		2. REPORT TYPE Annual		3. DATES COVERED 1 Dec 2008 – 30 Nov 2009	
4. TITLE AND SUBTITLE Mathematical Modeling of Physical and Cognitive Performance Decrement from Mechanical and Inhalation Insults			5a. CONTRACT NUMBER W81XWH-06-C-0051		
			5b. GRANT NUMBER		
			5c. PROGRAM ELEMENT NUMBER		
6. AUTHOR(S) James H. Stuhmiller E-Mail: James.Stuhmiller@L-3com.com			5d. PROJECT NUMBER		
			5e. TASK NUMBER		
			5f. WORK UNIT NUMBER		
7. PERFORMING ORGANIZATION NAME(S) AND ADDRESS(ES) L-3 Services, Inc. San Diego, CA 92121			8. PERFORMING ORGANIZATION REPORT NUMBER		
9. SPONSORING / MONITORING AGENCY NAME(S) AND ADDRESS(ES) U.S. Army Medical Research and Materiel Command Fort Detrick, Maryland 21702-5012			10. SPONSOR/MONITOR'S ACRONYM(S)		
			11. SPONSOR/MONITOR'S REPORT NUMBER(S)		
12. DISTRIBUTION / AVAILABILITY STATEMENT Approved for Public Release; Distribution Unlimited					
13. SUPPLEMENTARY NOTES					
14. ABSTRACT This report describes specific accomplishments of Task Area K: Injury and Physiological Response to Blast, Blunt Trauma, and Inhaled Toxic Gases. Advances in mathematical modeling of injury and acute physiological response are described. Animal studies to determine critical model parameters and to collect data for validation of mathematical models are described. Advances in test instruments are also addressed. The report covers research conducted directly for the Military Operational Medicine Research Program and in collaboration with other civilian and military agencies.					
15. SUBJECT TERMS Blast, Overpressure, Injury, Modeling, Blunt trauma, Inhalation toxicology					
16. SECURITY CLASSIFICATION OF:			17. LIMITATION OF ABSTRACT UU	18. NUMBER OF PAGES 63	19a. NAME OF RESPONSIBLE PERSON USAMRMC
a. REPORT U	b. ABSTRACT U	c. THIS PAGE U			19b. TELEPHONE NUMBER (include area code)

Contents

	<u>Page</u>
1. INTRODUCTION	1
2. RESEARCH AREAS	5
2.1 INHALATION TOXICOLOGY RESEARCH	5
2.1.1 Development of a Fatigue Model & Blood Oxygen-based Parameter Correlates	5
2.1.2 Exercise Response Model.....	7
2.1.3 Physiologically Based Performance Model (PBPM) (Integrated Physiologic Fatigue Model)	9
2.1.4 TGAS 2.0P V&V package.....	12
2.1.5 The effect of hypoxia and carboxyhemoglobin concentration on exercise performance in goats	13
2.1.6 Toxic Gas Assessment Software PE v1.0.....	15
2.1.7 Updated TGAS Correlations with TGAS PE 1.0	18
2.1.8 Ventilation Response to O2, CO2, CO.....	21
2.2 ADVANCED BLAST TEST DEVICE (ABTD)	25
2.2.1 Development of Advanced Blast Test Device (ABTD)	25
2.3 HEAD INJURY	27
2.3.1 ECE Motorcycle Helmet Standard Evaluation (NHTSA Agreement)	27
2.4 HELMET MOUNTED SENSOR SYSTEMS.....	29
2.4.1 Finite Element Model (FEM) – Forward Modeling	29
2.4.2 Finite Element Model (FEM) – Reconstruction	31
2.4.3 Testing	33
2.4.4 HMSS Field Data Organization.....	35
2.5 BLAST BEHIND ARMOR	38
2.5.1 INJURY-A Development (NSRDEC ATO).....	38
2.5.2 MBTD Tests and Data Screening Software (NSRDEC ATO).....	40
2.5.3 Sheep Blast Test Device (SBTD) Tests (NSRDEC ATO)	42
2.5.4 Sheep Tests and FEM Development (NSRDEC ATO).....	44
2.6 BEHIND ARMOR BLUNT TRAUMA.....	45
2.6.1 Blunt Trauma Assessment Tools	45
2.7 ANTHROPOMORPHIC TEST DEVICE EVALUATION	48
2.7.1 THOR Dummy Air Bag Tests (NHTSA Agreement)	48
2.8 DATA PRESERVATION	49
2.8.1 Historical Data Recovery and Bowen’s Test Data Analysis	49
2.8.2 INJURY 8.3 in Simulink with Lethality Correlation	51
3. PRODUCTS	53
4. REFERENCES	55

Illustrations

<u>Figure</u>	<u>Page</u>
1. A diagram depicting the four possible states of motor units in the developed muscle model.	5
2. Estimated quadriceps muscle force during maximal functional electrical stimulation (FES) and the fitted curves.	6
3. Best fit regressions for four possible oxygen-related blood correlates to the recovery parameter R normalized to normoxic values for goats.	7
4. Ventilatory response to exercise (50% VO ₂ max).	8
5. Model results (-●-) compared to experimental data (grey with ±SD error bars) at steady state from workloads of 0, 60, 120, 180, and 240 W in normoxia. Data from [Wagner, Gale et al.1986].	9
6. Model prediction plotted against steady state experimental data obtained from exercising goats.	10
7. Performance decrement predictions plotted against experimental data from goat due to low oxygen and inhalation of carbon monoxide.	11
8. Performance decrement predictions plotted against experimental data for man sprinting in normoxic and hypoxic conditions. Data from [Weyand, Lee et al.1999].	11
9. Schematic of input and output files to run TGAS2.0P	12
10. Schematic drawing of the experimental setup.	13
11. Linear regressions of relationships between fractional VO ₂ max as a function of fractional C _a O ₂ with C _a O ₂ altered due to hypoxia (solid), [HbCO] (long dashed), hypoxia with hypercapnia (short dashed) and hypoxia and [HbCO] combined (dotted).	14
12. Main application window with “About” window visible.	16
13. Gas Exposure Pane.	17
14. Main application window after running model.	18
15. Histograms plotted to obtain a probability correlation of internal dose to the studied outcome.	19
16. Exposure-response curves to carbon monoxide inhalation for rat.	20
17. Combined effects of carbon monoxide and hydrogen cyanide.	20
18. Normalized ventilatory response of rat to a 10-minute exposure to oxygen.	23
19. Normalized ventilatory response of rat to a 5-minute exposure carbon dioxide.	24
20. Normalized ventilatory response of rat exposed carbon monoxide.	25

21.	ABTD front view.....	26
22.	ABTD side view.Modular sensor panels shown.....	26
23.	ECE free drop fixture.....	28
24.	ECE anvils.	28
25.	ECE skull fracture comparison with acceleration.....	28
26.	ECE skull fracture comparison with HIC.	29
27.	Finite element model of helmet and headforms.....	30
28.	Forward modeling analysis.	30
29.	Accuracy of FEM prediction.	31
30.	Offset seen in external HMSS sensors.....	32
31.	Calculated head injury metrics using external mounted sensor.....	33
32.	Calculated head injury metrics using internal mounted sensor	33
33.	Sample setup for a pendulum and shock tube impact.....	34
34.	Helmet and head acceleration – shock tube.....	34
35.	Helmet and head acceleration – air gun projectile.....	35
36.	Relational databases for field data.	36
37.	Field data directory structure.	37
38.	INJURY-A schematics.....	39
39.	Force balance on armor material.....	39
40.	INJURY-A data comparison.....	40
41.	MBTD and sensor schematics.	41
42.	MBTD with armor.	41
43.	Screening of data outliers.....	42
44.	Sheep Blast Test Device.	43
45.	Test results showing no significant differences in pressure data from SBTD and BTD.....	43
46.	Frontal compression test.	44
47.	Frontal compression data at 8m/s.	44
48.	Three-point rib bending test.....	45
49.	Schematics of the research method to accurately predict lung injuries due to blunt impacts.	45
50.	Detailed finite element model of swine lungs and their incorporation in swine torso.....	46

51.	Determine lung tissue damage threshold based on advanced imaging processing, computer simulation and statistical analysis.	47
52.	High-level design of BTAT 1.0	47
53.	THOR-05F vs.Hybrid III for Aggressive Bag: head position at bag separation.	48
54.	THOR-05F vs.Hybrid III for Aggressive Bag: head position at bag.....	49
55.	Original Bowen's test conditions.	50
56.	Bowen's test set up.....	50
57.	Scaled Bowen's tests at sea level with same distances.	51
58.	Scaled Bowen's tests at sea level with same charge weights.....	51
59.	INJURY 8.3 in Simulink.....	52

1. Introduction

The Military Operational Medicine Research Program (MOMRP) of the US Army Medical Research and Materiel Command (USAMRMC) faces ever increasing pressure to answer more mission relevant questions with less resources and time. The Catch-22 aspect is that problems cannot be satisfactorily solved at the moment they arise unless the supporting research basis has already been laid. Consequently, it is imperative to be proactive: anticipate need and put in place the broadest infrastructure of applied research that can be practically accomplished.

This contract supports the MOMRP Research Area in Injury Prevention and Reduction. Specifically, the research supports Task Area K: “Injury and Physiological Response to Blast, Blunt Trauma, and Inhaled Toxic Gases.” This Task Area addresses the internal and external damage inflicted by the trauma of blast and blunt force and the acute physiological consequences of trauma and inhaled toxic gases. It captures the processes in mathematical models that support health hazard and survivability assessments and the evaluation and improvement of personnel protection systems.

Blast and blunt force thoracic trauma, including penetration wounding, are the greatest threats on the battlefield and their mitigation is one of the highest priorities of the Army. To design effective protection, without excessive operational burden, requires a quantitative knowledge of the mechanisms and threshold of injury.

Thoracic and pulmonary insults from blast, blunt trauma, or toxic gases can produce acute effects that vary from temporary disruption of physical and cognitive performance to complete incapacitation and death. The levels of exposure that produce incapacitation and death are generally known and these levels are used to set exposure limits and to estimate the consequence of injury. In many occupational situations and nearly all combat situations, the occurrence of physical or cognitive degradation can have nearly the same disastrous outcomes when the warfighter cannot take the proper actions for self protection. Estimation of these debilitating effects is less well known and is not known for combined trauma.

The goals of this Task Area are to describe the physical processes associated with the interaction of the external trauma source with personal protection and the body's biomechanical and physiological response in order to determine tissue level damage and whole body consequences of that damage. This information is used to develop, validate, and implement user-oriented application models of the critical physiological processes that are necessary to understand the response to thoracic and pulmonary trauma.

The human body is a complex, multi-level, composite mechanical structure that has properties and mechanical response characteristics that are highly interactive. Furthermore, the greatest knowledge of this mechanical structure has been derived from normal human activities, not for nonphysiological levels of stress and distortion. In addition, the rapidity, magnitude, and location of the military trauma are often quite different from that seen in civilian circumstances. Taken together, military blast and blunt force thoracic trauma pose problems that have not been previously studied or solved.

Concurrently with biomechanical responses, reduced physical and cognitive abilities are a result of physiological responses to the initial trauma. For example, inhalation of carbon monoxide can be characterized by the external gas concentration and duration of exposure, but the decrement in cognitive ability depends on the decrease in oxygen delivered to the brain, which depends on the competition with oxygen for hemoglobin, which in turn controls the body's reflex to increase ventilation and is affected by the presence of other gases that might increase or decrease this response. Furthermore, concurrent trauma, from a blast for example, might damage the air-blood barrier in the lung, further interfering with the body's ability to deliver oxygen to the brain. Adding the effects of altitude, which lowers the naturally occurring oxygen levels in the atmosphere, and exertion, which increases the demand for oxygen in other parts of the body, further alter the oxygen delivery to the brain and therefore the cognitive performance. Clearly, all of these physiological processes must be accounted for to have a generally valid means of estimating the effects of trauma.

The form of the model equations, the parameters needed by the models, the variation of parameters across species, and the experimental data to validate the models are found by extensive review of the literature. The overview is captured in source books. The references are placed in literature databases. The experimental data is digitized and placed in other data structures. A system of software allows validation calculations to be run for a wide range of tests and compared graphically to the test data.

When critical parameter values or validating test data are not available, focused animal tests are conducted to provide the missing information. The Task Area draws upon researchers at the University of California, San Diego and Davis for large animal tests of trauma response, exercise and performance, and advanced medical imaging; upon researchers at the Lovelace Institute for small animal studies under toxic and altitude conditions; at the Medical College of Wisconsin for post mortem human subject studies; and at USARIEM for companion studies in human volunteers.

The workhorse of thoracic blast and blunt force trauma modeling is Finite Element Analysis (FEA). FEA accounts for the complex geometrical and material property variations within the

body by breaking the body into hundreds of thousands of small elements, each with the correct shape, orientation, mechanical property, and connection to neighboring elements. Within each element, the fundamental rules of mechanics are applied. The result is a model that can represent the detail of the trauma delivered, the anatomy of the body, and the response of individual tissues and organs. The tissue damage criteria are valid for all species and therefore can be determined with animal tests. The models can be simplified and packaged as screening tools for end users.

Similarly, the workhorse of physiological modeling is Systemic Modeling. The body's major systems (respiration, circulation, and metabolism) form the main structure of the model. The humoral and neural control systems provide feedback and feedforward signals that try to keep the body functions in balance. Models of oxygen delivery, absorption, and support of ATP generation provide the bases of cognitive and physical performance. Blood chemistry determines the absorption, unloading, and transformation of internal and external chemical species. These models are formulated and solved in a state of the art simulation environment that allows arbitrary complexity and accurate solution. These response models provide the rational basis for health hazard and survivability assessments and protection system design.

The fundamental models of injury and physiological response are assembled into software applications for specific end user needs. Input formats are customized to the data formats of those users and output reports are customized to the particular analyses needed. In some instances, the software is formulated as modules that can be incorporated into other applications. The applications are upgraded as research progresses and will be accredited for defense-wide adoption.

Threats to the soldier are growing in nontraditional areas, such as acoustic, electromagnetic, ionizing radiation, chemical, and biological weapons. These threats have both a physical component (coupling of the external threat to the organs of the body) and a systemic effect (disruption of the normal protection and response functions). Although many of the physical interactions are known, they have never been combined with physiological response to produce a quantitative and predictive methodology. The infrastructure needed to allow the MOMRP to respond effectively should include these effects.

The MOMRP is a nexus for research on traumatic effects for a wide range of civilian and military organizations. MOMRP has collaborative research agreements with the National Highway Traffic Safety Administration, the Joint Non-Lethal Weapon Directorate, the Natick Soldier System Research and Engineering Center, and other agencies interested in expanding and applying the science of injury. The research findings from those collaborative efforts are also reported here.

The research conducted under this contract has provided critical hardware, software, and knowledge products to assist the MOMRP effort. This report summarizes those products in the following areas:

- ▶ Blast Injury Research
- ▶ Behind Armor Blunt Trauma Research
- ▶ Inhalation Toxicology Research
- ▶ Head and Neck Injury Research
- ▶ Distributed Thoracic Trauma Research
- ▶ Biomechanics Research
- ▶ Data Preservation

Much of the work has appeared in peer-reviewed journals. Key software products are distributed through the MOMRP web site. Critical hardware is used throughout the military for assessment. In our own small way, L-3/Jaycor has helped the Military Operational Medicine Research Program meet its objective that “MOMRP research touches every soldier, every day.”

2. Research Areas

2.1 INHALATION TOXICOLOGY RESEARCH

2.1.1 Development of a Fatigue Model & Blood Oxygen-based Parameter Correlates

Liu et al. (2002) introduced a muscle-based “phenomenological” model to predict exercise performance. The model takes into account the overall force generating capacity of muscle using only a few parameters that are based on muscle during activation properties. In order for the model to be practical under a wide range of protocols, it is of interest to determine how the model parameters change in the short-term, where environmental conditions such as hypoxia or toxic gas inhalation may alter fatigue and/or recovery mechanisms.

We expanded upon the model presented by Liu et al. (2002) and formulated an algorithm that allows the equations governing muscle activation to be solved if the desired force profile is known (Figure 1). In addition, we supported the validity of the phenomenological model by applying it to additional forms of human exercise, including cycling, running, and maximum quadriceps contractions (Figure 2). Finally, we explored the physical meanings of the parameters by looking at how they vary between runners with different specialties, and presumably, fiber types.

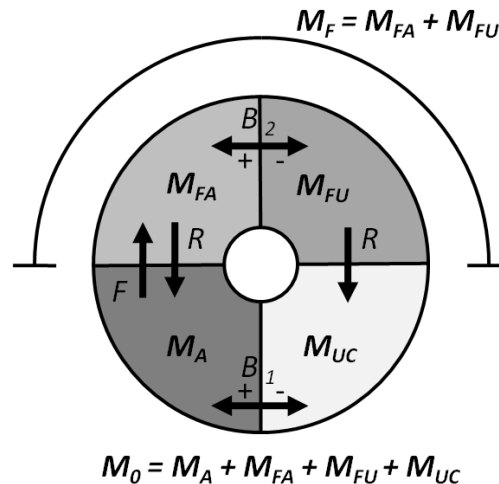


Figure 1. A diagram depicting the four possible states of motor units in the developed muscle model.

M_{uc} and M_A are inactive and active unfatigued fibers, respectively. Fatigued fibers can be active (M_{FA}) or inactive (M_{FU}). Only active unfatigued fibers (M_A) generate force and the total number of fibers (M₀) is the sum of the four fiber pools. Brain command (B₁ and B₂) determines whether fibers are active or inactive, regardless of fatigue status. Based on the model presented by Liu et al. (2002).

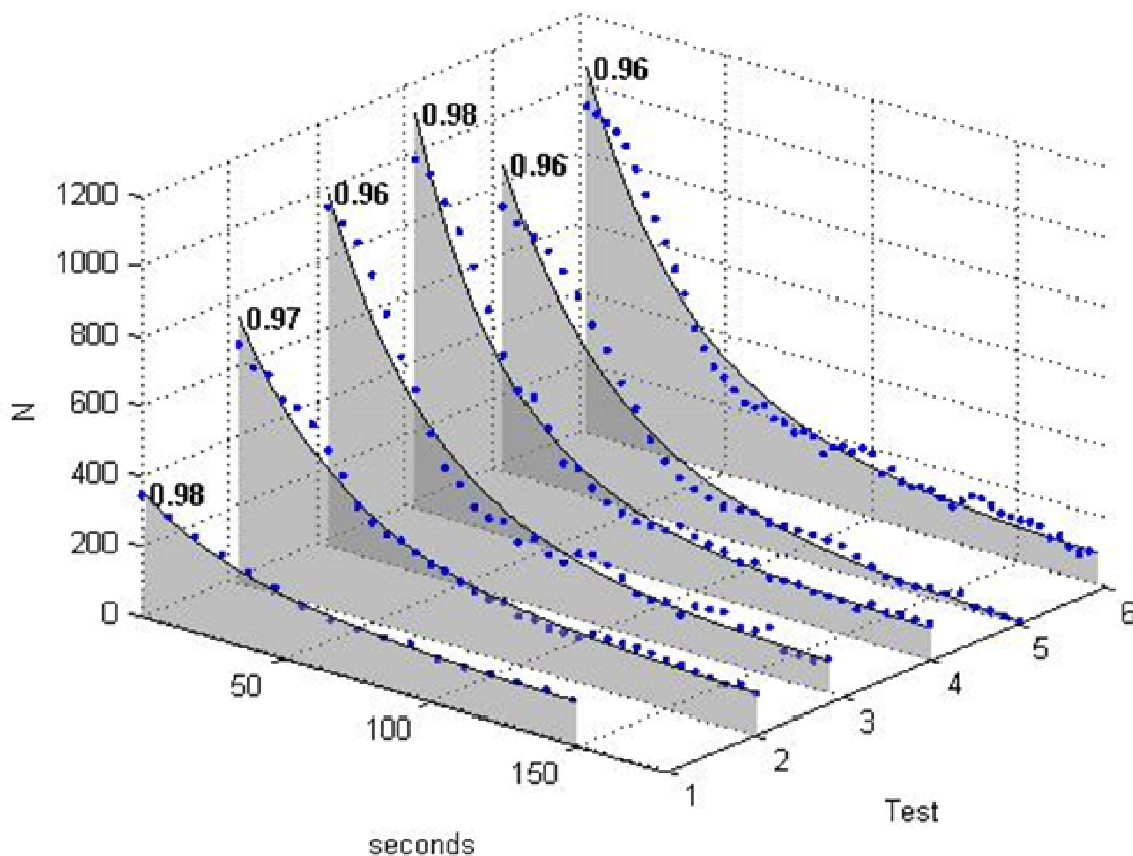


Figure 2. Estimated quadriceps muscle force during maximal functional electrical stimulation (FES) and the fitted curves.

The shaded areas represent individual data presented by various sources and the lines are the fitted model prediction. Bold numbers at the start of each test are R2 values and indicate the model is able to fit the data. Data from [Ding, Wexler et al. 2000], [Levy, Mizrahi et al. 1990], [Giat, Mizrahi et al. 1993].

To explore possible oxygen determinants of the recovery factor R , both time-to-fatigue and oxygen measures at different workloads need to be measured on the same subjects. Being unable to find human data of this type in the literature and the time consuming nature of this type of experiment, novel data was collected on goats rather than humans. After validating individual goat's parameter values under normoxic, hypoxic, and 30% [HbCO] conditions, a regression relating the recovery parameter to the blood measures SaO_2 , SvO_2 , PaO_2 , and PvO_2 was calculated (Figure 3). A similar regression for humans may be of value in predicting time to fatigue in toxic gas situations.

Goat experiments were carried out by the Equine Athletic Performance Lab at the University of California, Davis.

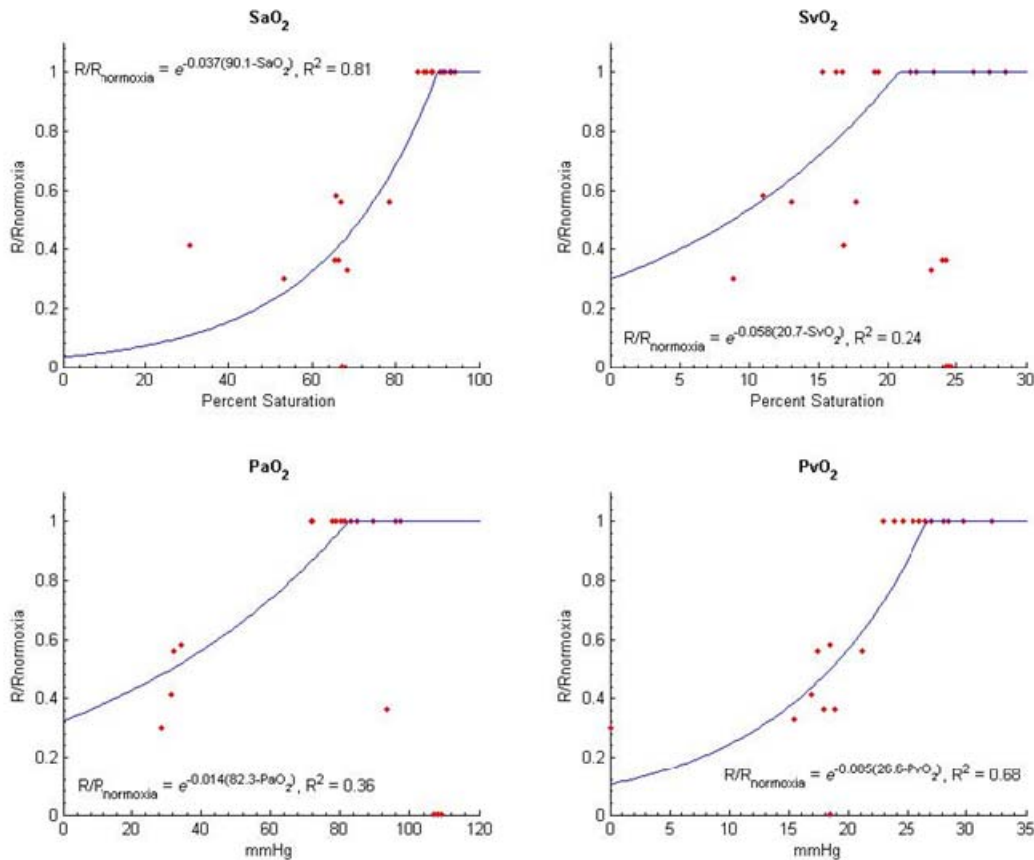


Figure 3. Best fit regressions for four possible oxygen-related blood correlates to the recovery parameter R normalized to normoxic values for goats.

SaO₂ had the highest R² followed by PvO₂. SvO₂ and PaO₂ had poor correlations due to the wide scattering of nonnormoxic data.

- | | |
|------------|--|
| Product 1. | Implemented fatigue model in Matlab for use in the Physiological-based Performance Model (PBPM). |
| Product 2. | Sih, B.L., Ng, L., and Stuhmiller, J.H. “Generalization of a ‘phenomenological’ muscle fatigue model.” Technical report J0287-10-382 (in preparation). |
| Product 3. | Sih, B.L., Ng, L., and Stuhmiller, J.H. “The effects of hypoxia and carboxyhemoglobin concentration on a ‘phenomenological’ model’s recovery parameter.” Technical report J0287-10-383 (in preparation). |

2.1.2 Exercise Response Model

An exercise response model has been developed to predict physiologic response to exercise not only in normal atmospheric conditions but also in low oxygen and carbon monoxide environments. The model builds upon the exercise ventilation module and muscle metabolism module. The modules are integrated into the Dynamic Physiologic Model (DPM), which

accounts for ventilatory response from chemoreceptors, to track oxygen consumption and carbon dioxide generation throughout the body during exercise.

The ventilatory response to exercise has been characterized by three phases. See Figure 4. Phase I, identified by an abrupt jump, is triggered by the onset of muscle movement. This abrupt jump has been attributed to afferent feedback and central command, which come from passive movement and active movement, respectively. Phase II, identified by a slow exponential rise to a new steady state (Phase III) for a constant workload, has been attributed to humoral control. In the model, humoral stimulation is dependent on a chemical factor that is released in proportion to the exercise level. As the muscle works, a number of chemicals and ions are released into the bloodstream and may trigger increased ventilation in order to meet oxygen demand and carbon dioxide generation. The ventilatory increase is divided so breathing frequency is increased by 75% and the remaining 25% of the increase goes to tidal volume.

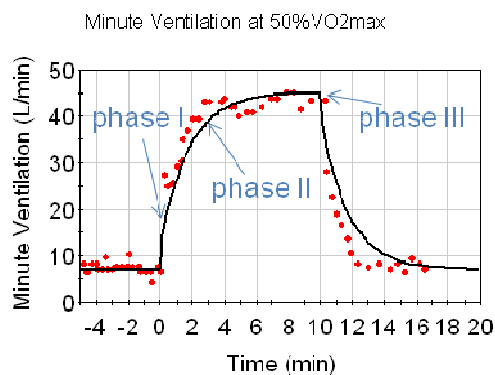


Figure 4. Ventilatory response to exercise (50% VO₂max).

An abrupt start on a treadmill produces an immediate jump in ventilation with a slow exponential rise to steady state. Data from [Mateika and Duffin 1992].

The muscle metabolism module calculates the amount of oxygen consumed and carbon dioxide generated as required by workload. The availability of oxygen in the tissue is dictated by the amount of oxygen diffused from the blood to the tissue. As work intensity increases, the required oxygen for aerobic work may exceed the amount of oxygen diffusing from the blood. At this point, anaerobic work makes up this difference. Lactate levels in the blood are dictated by the amount of anaerobic work.

Integration of the exercise ventilation response module, the tissue metabolism module, and the DPM model gives a whole body picture of physiologic response to exercise in normal and low oxygen as well as carbon monoxide filled environments. The model has been validated against blood chemistry and ventilatory variables for man. See Figure 5 for a comparison of model predictions to experimental data of measured external and internal physiologic variables.

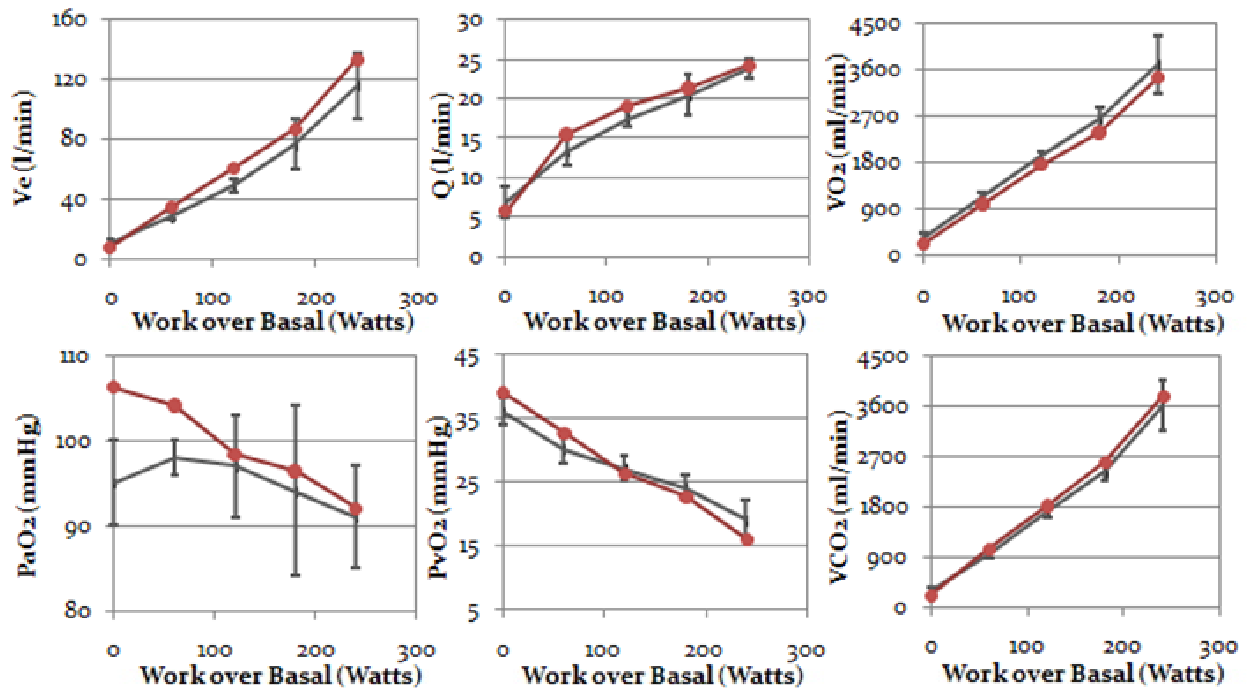


Figure 5. Model results (-•-) compared to experimental data (grey with \pm SD error bars) at steady state from workloads of 0, 60, 120, 180, and 240 W in normoxia. Data from [Wagner, Gale et al. 1986].

- Product 4. A model that predicts physiologic response to exercise.
- Product 5. Ng, L., Sih, B.L., and Stuhmiller, J.H. "A Model of Physiologic Response to Exercise." Technical report J0287-10-384 (in preparation).

2.1.3 Physiologically Based Performance Model (PBPM) (Integrated Physiologic Fatigue Model)

A Physiologically Based Performance Model (PBPM) has been developed to predict physical performance decrement when oxygen delivery has been compromised. To do this, a model of physiologic response to exercise and a model of muscle fatigue which have been developed and validated separately are integrated. Integration occurs through a relationship between the physiologic variable of arterial oxygen saturation (Hb_{ArtO_2}), which is calculated in the exercise response model, and the recovery parameter in the muscle fatigue model. A relationship between the two variables was identified through goat exercise and goat fatigue tests in hypoxic and carbon monoxide environments.

PBPM was validated against internal and external physiologic variables collected from steady state exercise goat data. Validation was run against exercise test data collected in 50%, 21%, 12%, and 9% O_2 as well as CO levels which produced 15%, 30%, and 50% COHb. See Figure 6 for validation in normoxia. This confirmed that the physiologic response to exercise in goat is correctly predicted, allowing use of the relationship between the blood chemistry varia-

ble, HbArtO2, and the recovery parameter of the muscle fatigue model to be implemented. The endurance predictions were validated against a matrix of 5 goats run to fatigue in normoxia, 12% O2, and at levels of CO which produced 30% COHb. See Figure 7. Finally, the endurance predictions were validated against data collected from man sprinting in 21% and 13% O2 (Figure 8).

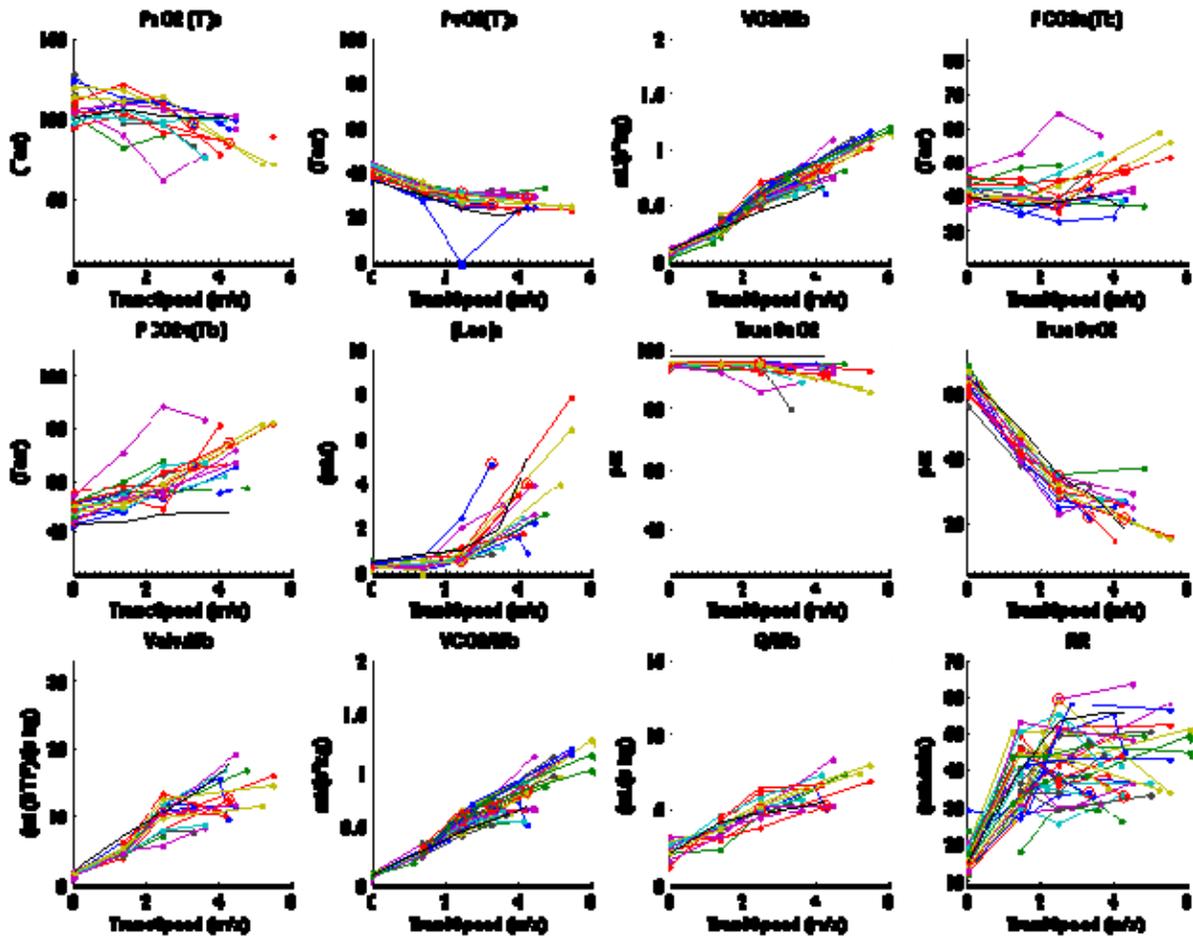


Figure 6. Model prediction plotted against steady state experimental data obtained from exercising goats.

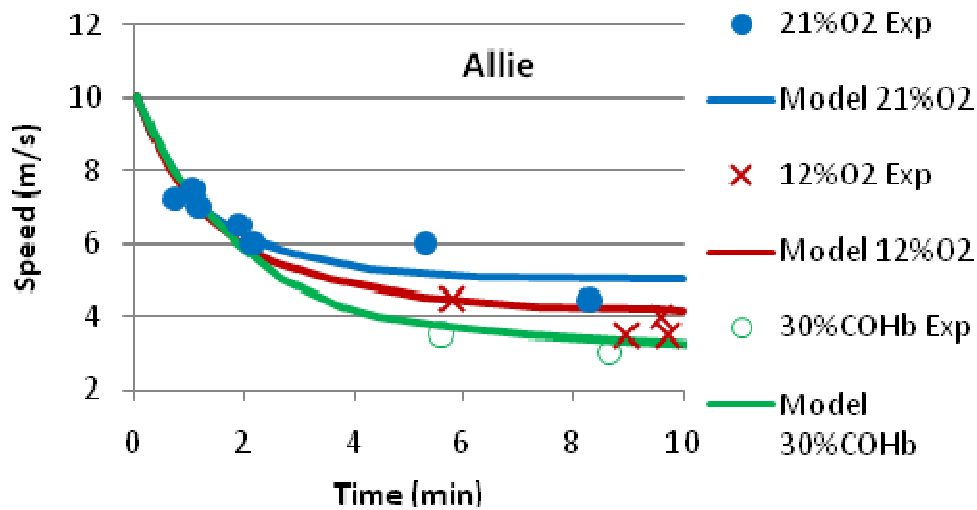


Figure 7. Performance decrement predictions plotted against experimental data from goat due to low oxygen and inhalation of carbon monoxide.

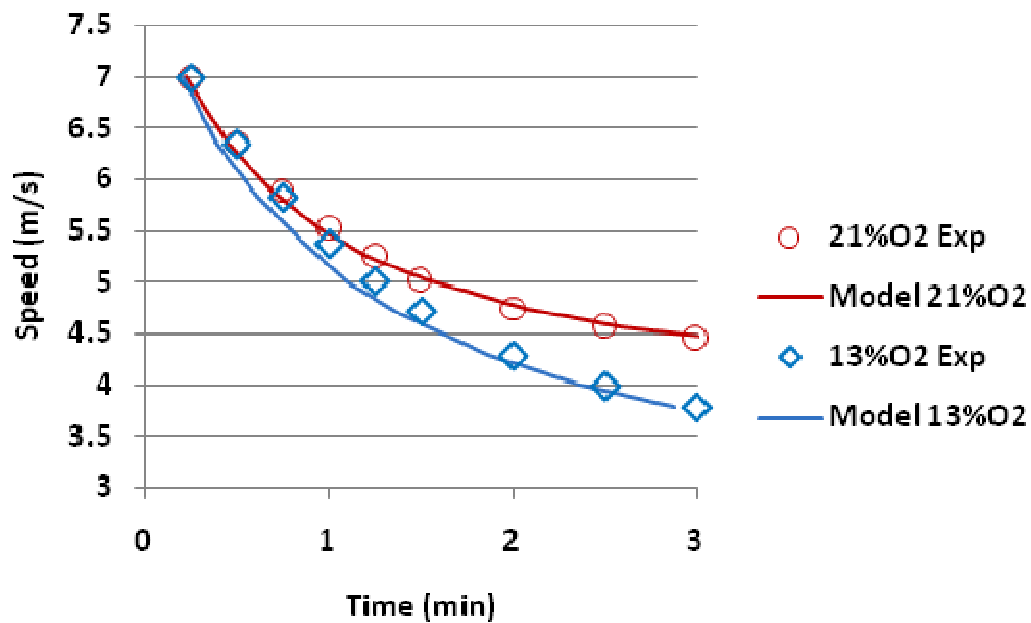


Figure 8. Performance decrement predictions plotted against experimental data for man sprinting in normoxic and hypoxic conditions. Data from [Weyand, Lee et al. 1999].

- Product 6. A model that predicts physiologic response and physical performance decrement due to low oxygen and carbon monoxide exposures.
- Product 7. Ng, L., Sih, B.L., and Stuhmiller, J.H. "A Physiologically Based Performance Model." Technical report J0287-10-385 (in preparation).

2.1.4 TGAS 2.0P V&V package

TGAS2.0P is an application designed to predict incapacitation, lethality, and secondary physiologic effects due to inhalation of fire and metabolized gases. A validation and verification (V&V) package was assembled for TGAS 2.0P in January 2009. The following items were included as part of the package:

- TGAS2P Documentation.doc: This summary document presents the theory and derivation of equations implemented by the model. A schematic depicting the flow of TGAS Inputs to Outputs is included. See Figure 9. Determination of critical endpoints (incapacitation, lethality, and secondary effects) is explained. Tables of key variables are included.

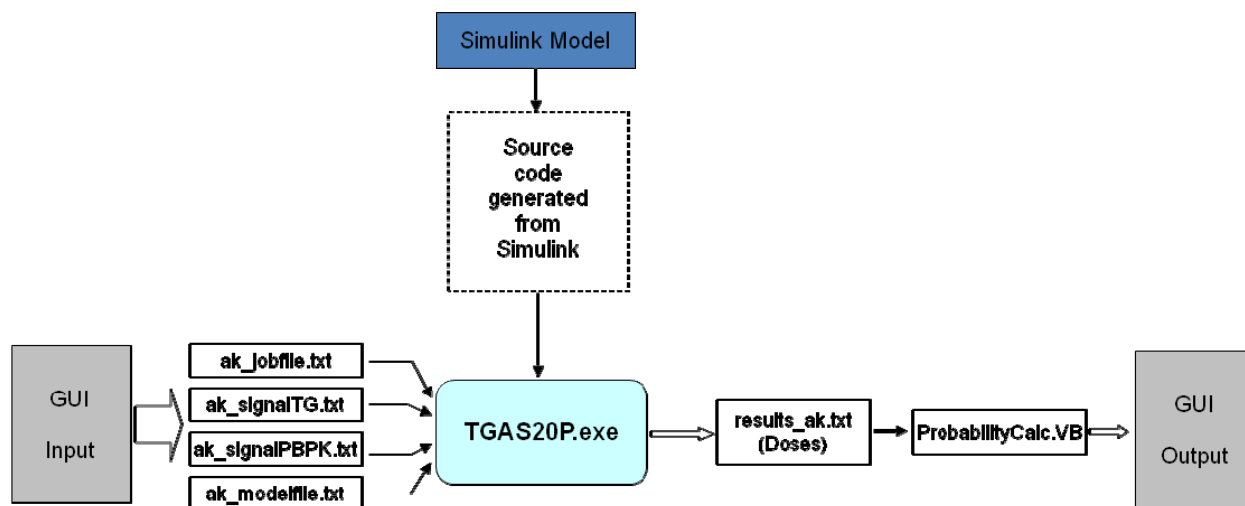


Figure 9. Schematic of input and output files to run TGAS2.0P

- CompiledCode.txt: This ANSI/ISO C++ code is generated from the Simulink Model through Matlab.
- AnnotatedCompiledCode.doc: The C++ code in 'CompiledCode.txt' is annotated to identify each line with the model equations in 'TGAS2P Documentation.doc'.
- TG20p.exe: The executable of TGAS 2.0P.
- Probabilities.bas: The script used to calculate the probabilities of incapacitation and lethality based on internal dose.
- TestCases Folder: Examples of test cases to run in the simulation. Test cases include exposure to fire gases (HCN, HCL, NO₂, CO, AC, low O₂) and twenty-one metabolized gases.

This package is awaiting accreditation from ARL/SLAD.

Product 8. TGAS 2.0P V&V package

2.1.5 The effect of hypoxia and carboxyhemoglobin concentration on exercise performance in goats

The purpose of this study was to quantify if and how exercise capacity and aerobic capacity are affected in goats while breathing hypoxic, and/or hypercapnic gases with or without breathing small amounts of carbon monoxide (CO) to raise their carboxyhemoglobin concentration ([HbCO]). The experiment matrix tested if and how different inspired fractions of oxygen (O₂) (6, 9, 12, 15, 21 and 50%), carbon dioxide (CO₂) (0 and 5%) and inspired CO producing elevated [HbCO] (0, 15, 30 and 45%) alone and in combination cause a dose-dependent response to VO_{2max} and treadmill speed eliciting VO_{2max} . An additional question addressed was whether endurance capacity (fatigue) is affected at exercise intensities above and below that eliciting VO_{2max} while breathing these inspired gas mixtures. To answer these questions, a cross-flow indirect calorimetry system was constructed to measure oxygen consumption and O₂-transport variables in goats exercising on a treadmill (Figure 10). Room air (F_IO₂ 21%), hypoxia (F_IO₂ 12%), elevated [HbCO] (30% [HbCO]) were administered to goats while they ran at speeds above and below the speed required to elicit VO_{2max} until exhaustion to quantify the effect of altered inspired gases and VO_{2max} on endurance capacity.

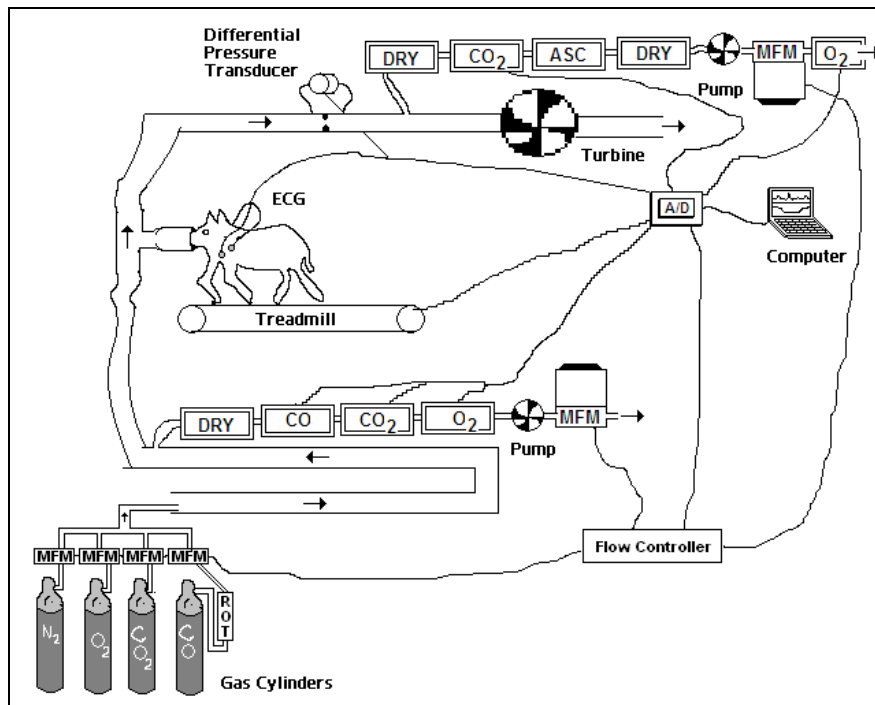


Figure 10. Schematic drawing of the experimental setup.

CO₂, O₂ and CO are gas analyzers measuring the fraction of the respective gas. DRY and ASC are Drierite and Ascarite used to remove where water vapor and CO₂ from the measuring system, respectively. MFM is a mass flow meter that measured flow and that was set by the flow controller. ROT is a rotameter that measured flow and was controlled by a needle valve, ECG is electrodes and an amplifier for recording the electrocardiogram and A/D is an analog-to-digital converter for sending data to the computer on which they were stored.

Both hypoxia and elevated [HbCO] decreased VO_{2max} and running speed at VO_{2max} in a dose-dependent manner while hyperoxia and hypercapnia showed no significant differences from room air (21% O_2). Hypoxia and elevated [HbCO] both decrease arterial O_2 concentration (C_aO_2), albeit by different mechanisms – decreased O_2 saturation of Hb binding sites vs. decreased capacitance of the Hb to bind O_2 . At speeds eliciting VO_{2max} , no significant differences ($P = 0.54$) were found between the slopes of the regression lines for VO_{2max} and C_aO_2 for hypoxia, hypoxia with hypercapnia, elevated [HbCO] and hypoxia with elevated [HbCO] (Figure 11). Neither hypoxia nor elevated [HbCO] resulted in any significant decreases in cardiac output (Q), suggesting that Q is unchanged at maximal exercise regardless of inspired gas concentrations despite a 60% decrease in VO_{2max} . Finally, lowering VO_{2max} shifts the speed vs. endurance time relationship (fatigue runs) as time to fatigue was shortened at the same absolute VO_2 when the goats breathed hypoxic gas and/or elevated [HbCO]. Results from the study suggest exercise capacity can be predicted from $F_I O_2$ and [HbCO] and can be used in developing rationally-based triage plans for protecting individuals, specifically soldiers and emergency personnel, exposed to these environments.

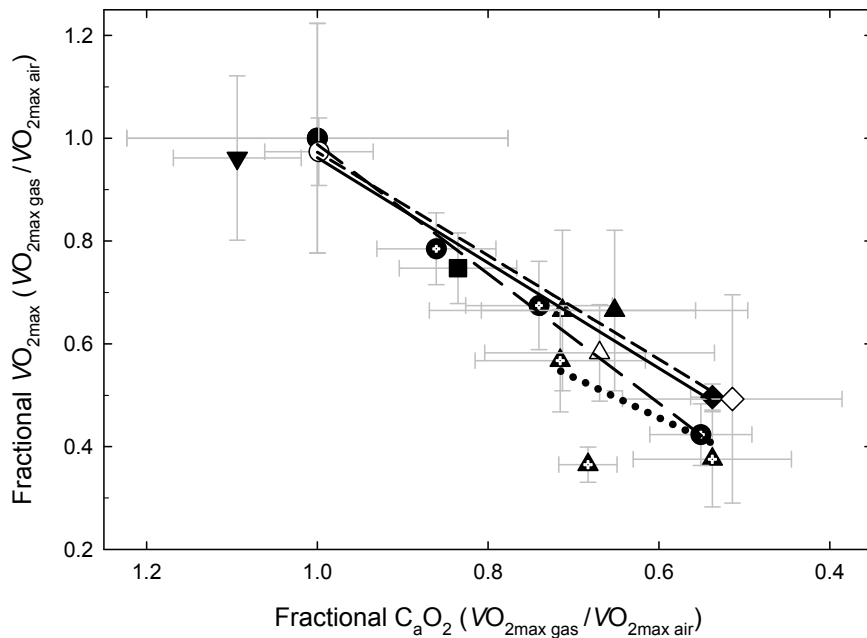


Figure 11. Linear regressions of relationships between fractional VO_{2max} as a function of fractional C_aO_2 with C_aO_2 altered due to hypoxia (solid), [HbCO] (long dashed), hypoxia with hypercapnia (short dashed) and hypoxia and [HbCO] combined (dotted).

Different $F_I O_2$ are denoted by different shapes (50% downward triangle, 21% circle, 15% square, 12% triangle and 9% diamond). A cross over the symbol denotes elevated [HbCO]; filled symbols are normocapnic and open symbols are hypercapnic gas (5% $F_I CO_2$). Individual points are the mean \pm SD for each gas mixture. Slopes of the lines were not different when tested by analysis of covariance whether the three long lines were tested ($P = 0.54$) or all four lines were tested ($P = 0.79$).

Experiments were carried out by the Equine Athletic Performance Lab at the University of California, Davis and delivered to L-3 Communications for organization and consolidation.

- | | |
|-------------|---|
| Product 9. | Crocker, G. H. (2010). "Effect of hypoxia, hyperoxia, hypercapnia and elevated carboxyhemoglobin concentration on VO ₂ max and exercise capacity in goats." University of California, Davis. |
| Product 10. | Crocker, G. H., Hayes, M. V., Weems, R. E., & Jones, J. H. 2008. "Effects of hypoxia on VO ₂ max and lactate accumulation rate in exercising goats." <u>The American Physiological Society Intersociety Meeting: The Integrative Biology of Exercise-V. 9-24-2008.</u> |
| Product 11. | Kwon, J., Crocker, G. H., Jones, E. M., Nye, S. M., Perloff, S. H., Hayes, M. V., Toth, B., & Jones, J. H. 2009. "Does CO Binding of Hemoglobin Affect the Ventilatory Responses to Hypoxia, Hypercapnia or Both Ventilatory Stimulants?" <u>UC Davis School of Veterinary Medicine STARs in Science Student Research Symposium. 9-30-2009.</u> |
| Product 12. | Matlab-based access to organized and consolidated physiological and blood chemistry parameters for steady-state and fatigue runs |

2.1.6 Toxic Gas Assessment Software PE v1.0

Toxic Gas Assessment Software PE v1.0 is an incremental software release of the corresponding TGAS PE Inhalation Simulink Model being developed by L-3/Jaycor. The software provides a front-end (GUI) to the customer with a wide range of input options. TGAS PE v1.0 is built on the .NET framework 3.5 and can be run on all current versions of Microsoft Windows (including XP, Vista, and 7). The software provides an interface for the user to specify all relevant input information to the model (Figure 12). The user can specify exposure levels of all 31 gases that the model currently evaluates (Figure 13). The software also provides an interface to set the workload of the subject being evaluated. This is configured by using a set of predefined profiles (Inactive, light activity, etc.) or by defining a custom profile.

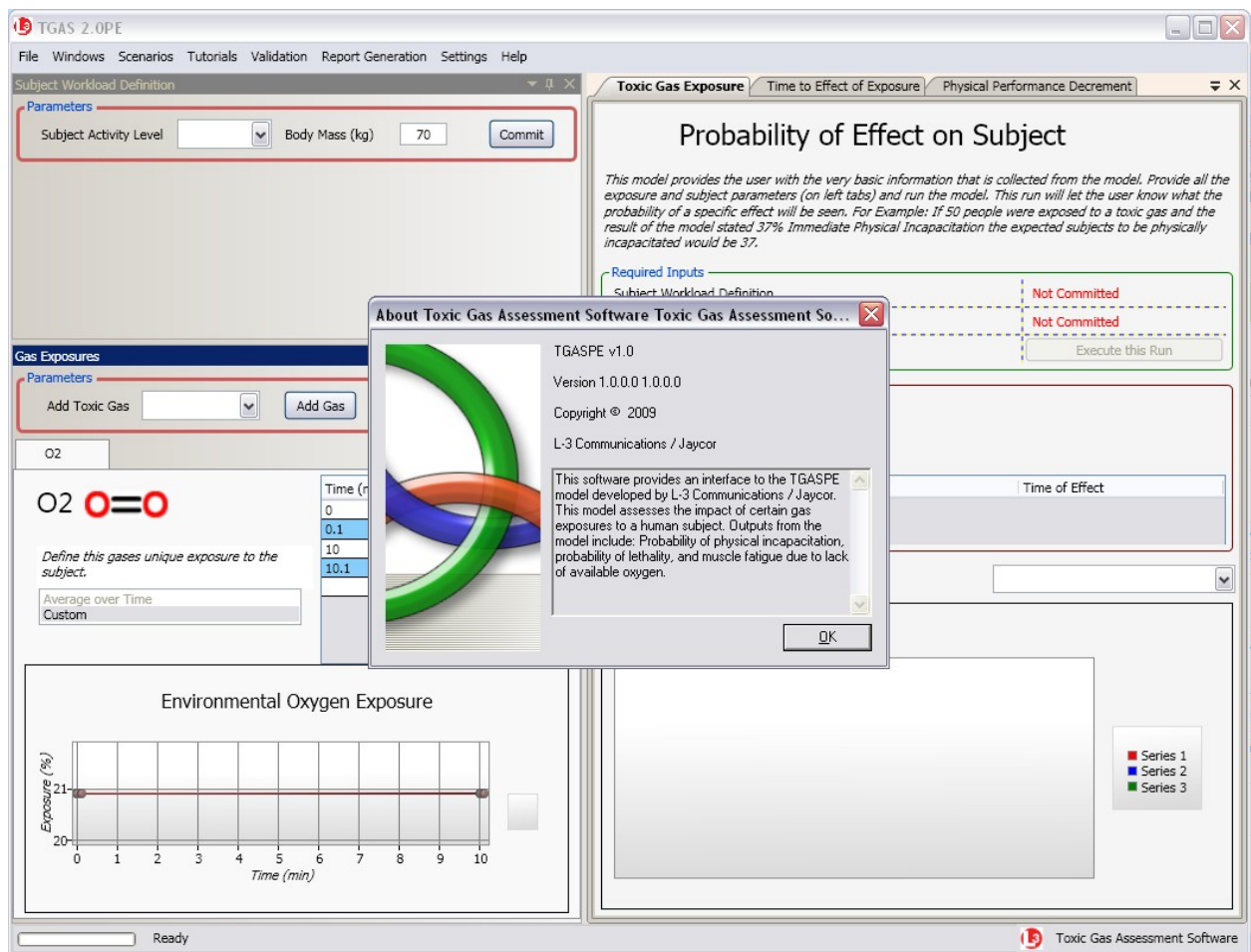


Figure 12. Main application window with “About” window visible.

This is the standard view of the application. To the left are the input window panes (Subject Workload Definition and Gas Exposures). To the right are the three main model simulations (Toxic Gas Exposure, Time to Effect of Exposure, Physical Performance Decrement).

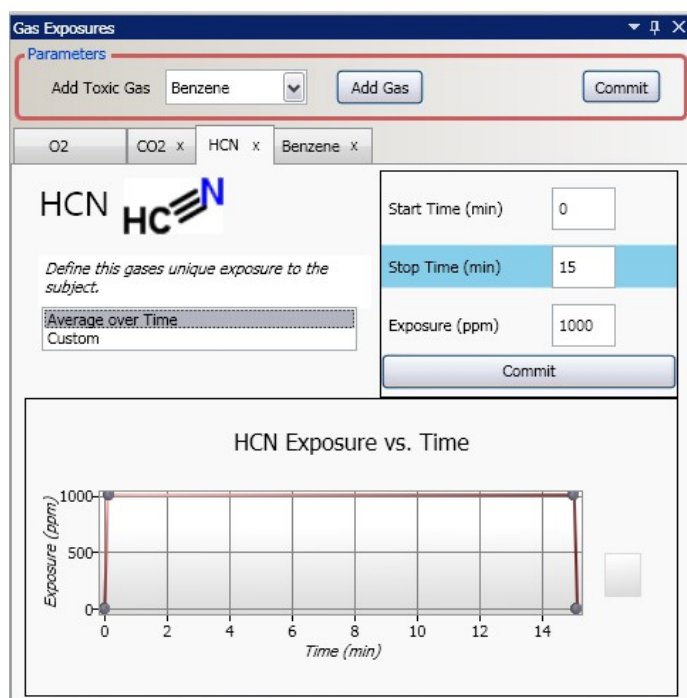


Figure 13. Gas Exposure Pane.

This is where the user defines the gas exposures to be input into the model.

The software provides facilities to visualize the results of the model. The user can view the internal dose of a specific gas in the subject, or view the probability of lethality or incapacitation over the time of the exposure (Figure 14). The software has been developed to ease the customer's use of the model and to provide insight on the ever expanding uses of the model as it continues to mature. The current software package provides an interface to investigate the "Probability of Effect due to an Exposure," "Time to Effect during an Exposure," and "Performance Decrement due to Exposure." Model runs can be saved and loaded for future investigation and output of the model can be exported in an Excel readable data file.

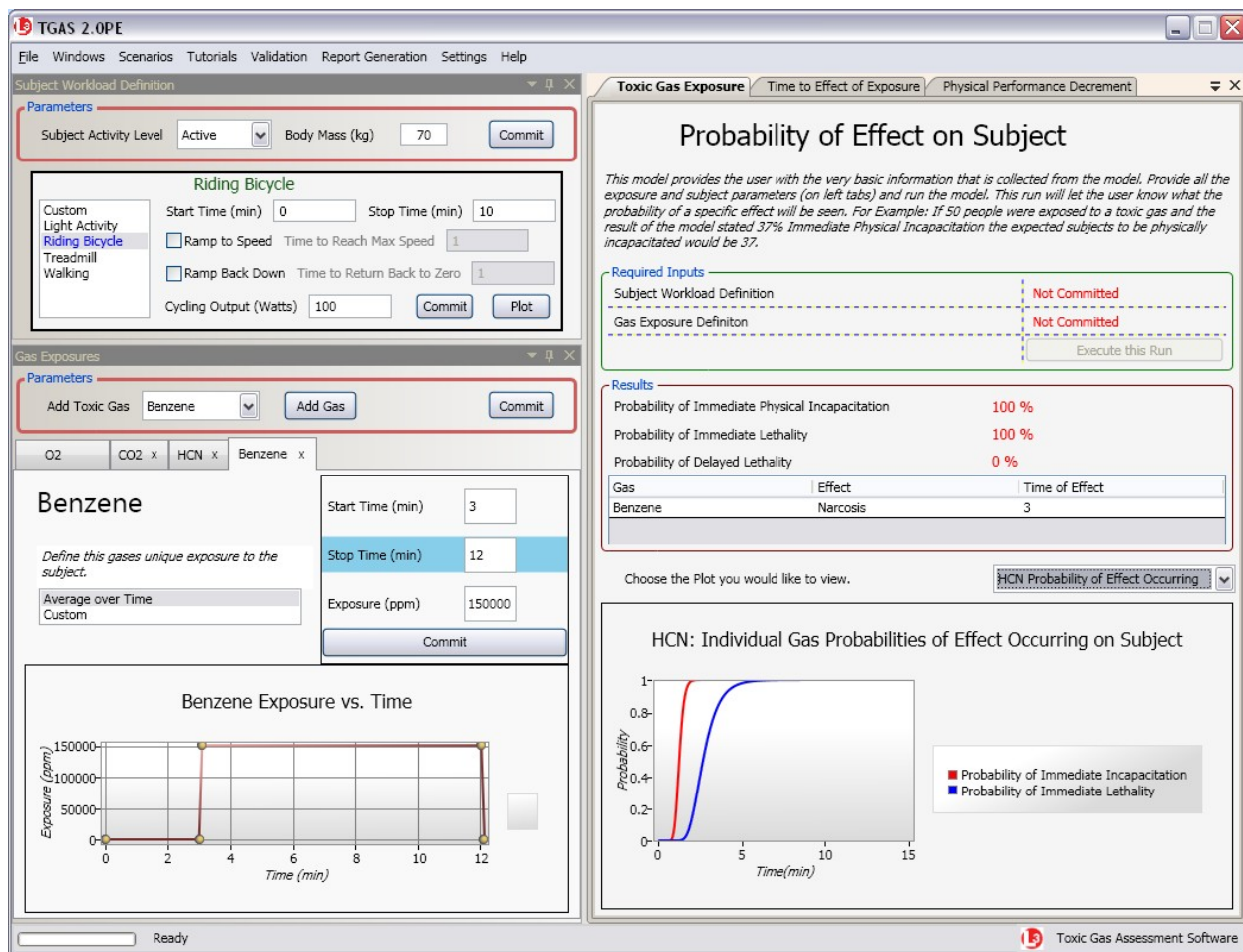


Figure 14. Main application window after running model.

The right side illustrates some of the available results.

The application has been validated against the Simulink Model to ensure that the proper calculations and output are being made.

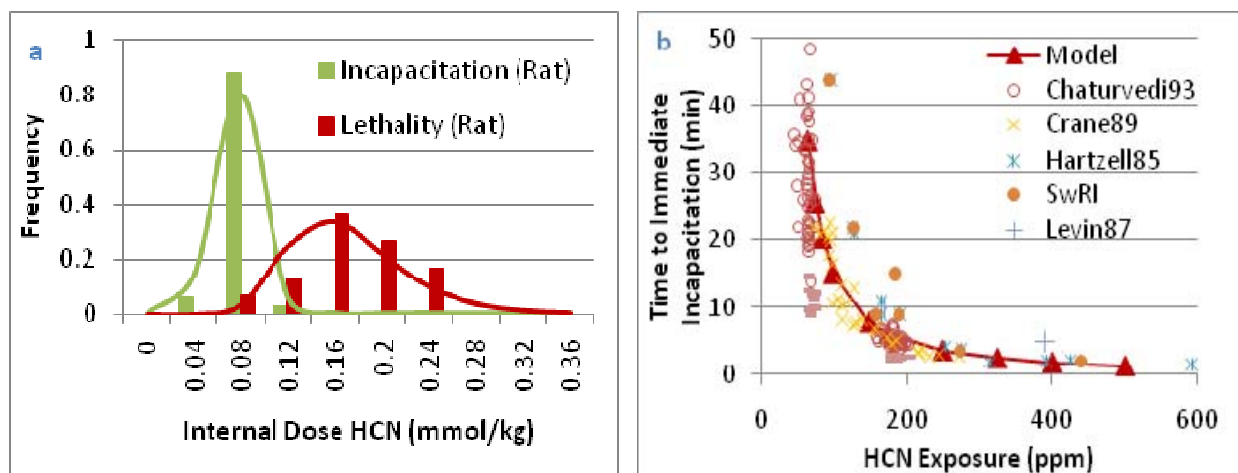
Product 13. Toxic Gas Assessment Software PE v1.0

2.1.7 Updated TGAS Correlations with TGAS PE 1.0

TGAS 2.0 has been revised to TGAS PE 1.0 to include a more physiologic ventilatory response module, tissue metabolism module, and muscle fatigue module. Accurate blood chemistry calculates the total concentration, partial pressure, and amount of oxygen, carbon dioxide, and carbon monoxide in plasma and bound to hemoglobin. Peripheral and central chemoreceptors to partial pressure of CO₂ in the arteries and cerebral spinal fluid, respectively, trigger ventilation response. In addition, ventilation is stimulated through increase in physical activity. The irritant fire gases trigger an immediate reflexive ventilatory response. These mechanisms are

implemented to produce a physiologically based ventilatory response to provide a more accurate calculation of internal dose.

The correlations of internal dose to an outcome of incapacitation and lethality due to inhalation of fire gases (low O₂, CO, HCL, HCN, NO₂, AC, and CO₂) are revisited with this model. A set of experimental data of exposure concentration and exposure time for certain outcome is run through the model to get a set of corresponding internal doses. A histogram is plotted to obtain a probability correlation of internal dose to the studied outcome. See Figure 15a. The dose at which there is a 50% probability of incapacitation or lethality is used to plot the model against exposure-response data. See Figure 15b and Figure 16. Finally, a combined exposure effect is examined for CO-HCN (Figure 17), CO-AC, and CO-HCL. All model predictions show good agreement with experimental data for rat.



(a) Histogram of calculated internal dose that led to incapacitation or lethality in rats.

(b) Exposure-response curves to hydrogen cyanide inhalation for rat (right).

Figure 15. Histograms plotted to obtain a probability correlation of internal dose to the studied outcome.

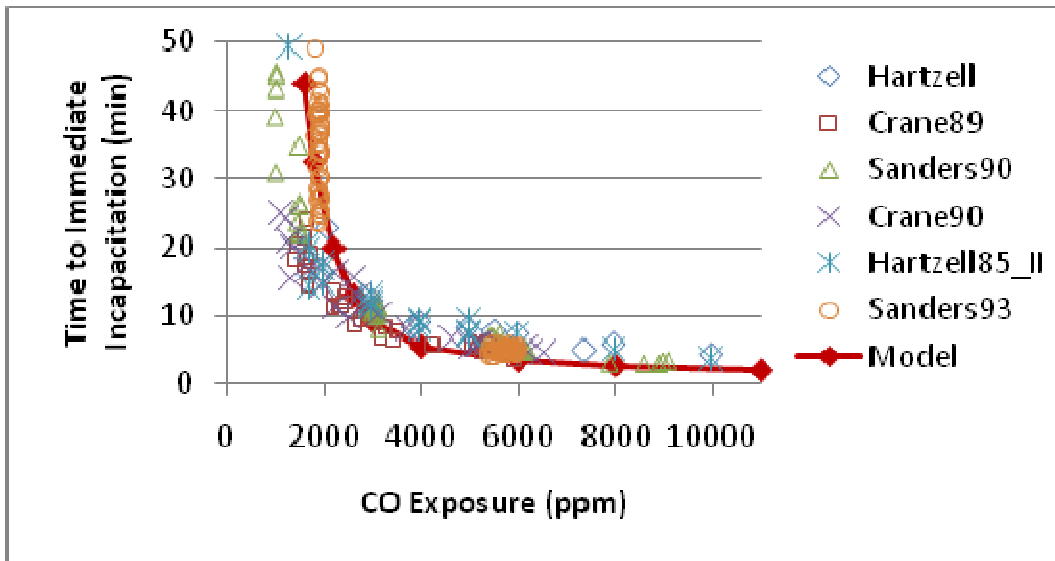


Figure 16. Exposure-response curves to carbon monoxide inhalation for rat.

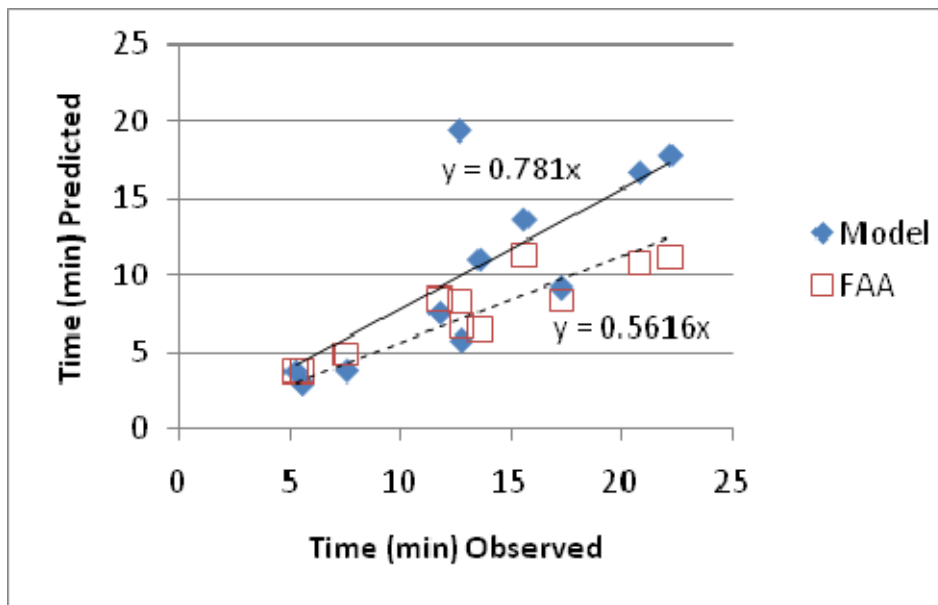


Figure 17. Combined effects of carbon monoxide and hydrogen cyanide.

Comparison of the model's predicted time to incapacitation vs. observed time to incapacitation. The model's prediction is also compared against the FAA fractional effective dose model.

The correlation to incapacitation for oxygen is based on availability of oxygen as determined from arterial oxygen saturation.

Product 14. A physiologic ventilatory response model integrated with the internal dose calculation for inhaled toxic gases.

2.1.8 Ventilation Response to O₂, CO₂, CO

Ventilation is the first step in providing oxygen to the body and the last step in eliminating carbon dioxide. As a result, the body has evolved a chemoreceptor system to control ventilation based on the sensed level of these blood gases. The peripheral receptors are located in the carotid and aortic bodies and the central receptors are located in the ventral medulla [Boggs 1991]. These sensors respond to changes in pH in the receptor tissues, which is normally controlled by carbon dioxide partial pressure, and the response is modulated by the hemoglobin saturation, which is normally controlled by oxygen partial pressure.

Several circumstances can alter blood gas levels and, thus, trigger a ventilation response. These circumstances include hypoxic or hypercapnic external atmospheres, altitude, respiratory distress, reduction in blood flow, and inhalation of toxic gases that interfere with the oxygen carrying capacity of hemoglobin. Under mild challenges, the chemoreceptor system can command ventilation changes that will bring the body back to normal conditions.

Under extreme conditions, the ventilation increase cannot adequately compensate and acute, deleterious effects can result. As the challenge is increased, these effects produce cognitive decrement, physical performance decrement, incapacitation, irreversible tissue damage, and eventually death. In those circumstances where the onset of oxygen deprivation is rapid, such as explosive decompression or exposure to fire gases, the response time of the ventilation control system, as well as the magnitude of the challenge, becomes critical. In some cases, the external atmosphere contains a mixture of gases, which further complicates the physiological response.

A quantitative understanding of the ventilation response and the subsequent ability of the body to retain adequate oxygen supply is critical to setting exposure standards, developing protective gear, assisting diagnosis, and interpreting physiological response. Being able to estimate these ventilation changes based on physiological processes is an important factor in correctly extrapolating immediate respiratory responses from animal to man. Mathematical models of the physiological systems can help achieve these goals.

There are three categories of mathematical models of the chemoreceptor control system: those aimed at explaining the response to hypoxia and hypercapnia; those aimed at explaining the effects of exercise; and those aimed at explaining the occurrence of periodic breathing, sleep apnea, and the stability of respiration. A considerable body of work has been developed as these models have evolved and some of the major contributors to the first category of models include Grodins [Grodins 1964; Grodins, Buell et al. 1967; Grodins and Yamashiro 1973], Duffin [Duffin and McAvoy 1988; Duffin 1989; Duffin 1991; Duffin 1994; Duffin, Mohan et al. 2000], Chiari [Chiari, Avanzolini et al. 1997], Longobardo [Longobardo, Cherniack et al. 1980; Longobardo, Gothe et al. 1982; Longobardo, Evangelisti et al. 2001; Longobardo, Evangelisti et

al. 2003], Ursino [Ursino, Magosso et al. 2001; Ursino, Magosso et al. 2001; Ursino and Magosso 2004], and their collaborators. There are also several excellent reviews of this field [Chang and Paiva 1898; Swanson, Grodins et al. 1898; Fidone and Gonzales 1986; Fitzgerald and Lahiri 1986; Whipp 1987; Boggs 1991; Honda, Miyamoto et al. 1992; Dempsey and Pack 1994; Hlastala and Berger 2001].

Building on this substantial base, the current authors produced the Dynamic Physiological Model (DPM) that incorporated the best aspects of previous work [Stuhmiller and Stuhmiller 2005]. The model was compared with data collected in goat exposed to high levels of carbon monoxide [Doblar, Santiago et al. 1977]. The model successfully captured transient dynamics of blood flow and blood chemistry in the brain, in particular, the quantities which drive the central chemoreceptors. In addition, the model captured the rapid ventilation increase that occurs when carboxyhemoglobin levels reached about 60% and the subsequent rapid decrease that follows from further exposure. The ventilation increase is explained by the oxygen deprivation in the brain, which leads to the onset of anaerobic metabolism that, in turn, creates an acidic environment that triggers a demand by the central chemoreceptors located in the ventral medulla. The subsequent ventilation decrease is explained by the failure of anaerobic metabolism to meet brain oxygen needs and the shutting down of central control processes. The mechanisms by which the control of breathing in affected that were hypothesized by Doblar are quantitatively confirmed by the model.

Although the DPM successfully captured the transient ventilation, as well as the underlying mechanisms, as observed in these particular goat studies, it is important to determine if the model remains valid for other species and for a wider range of gases and combinations. A companion research program, conducted at the Walter Reed Army Institute of Research (WRAIR), provides quantitative ventilation response data in rat to acute exposures to oxygen (Figure 18), carbon dioxide (Figure 19), carbon monoxide (Figure 20), and combinations of these gases.

A manuscript is being prepared that reports the comparison of the Dynamic Physiology Model (DPM) against the ventilation data man and rat over a wide range of exposures. The implications for the use of animal tests in the study of breathing control, the effect of fire gases on ventilation and toxicity, and the further understanding of the mechanisms of the central chemoreceptor will be discussed.

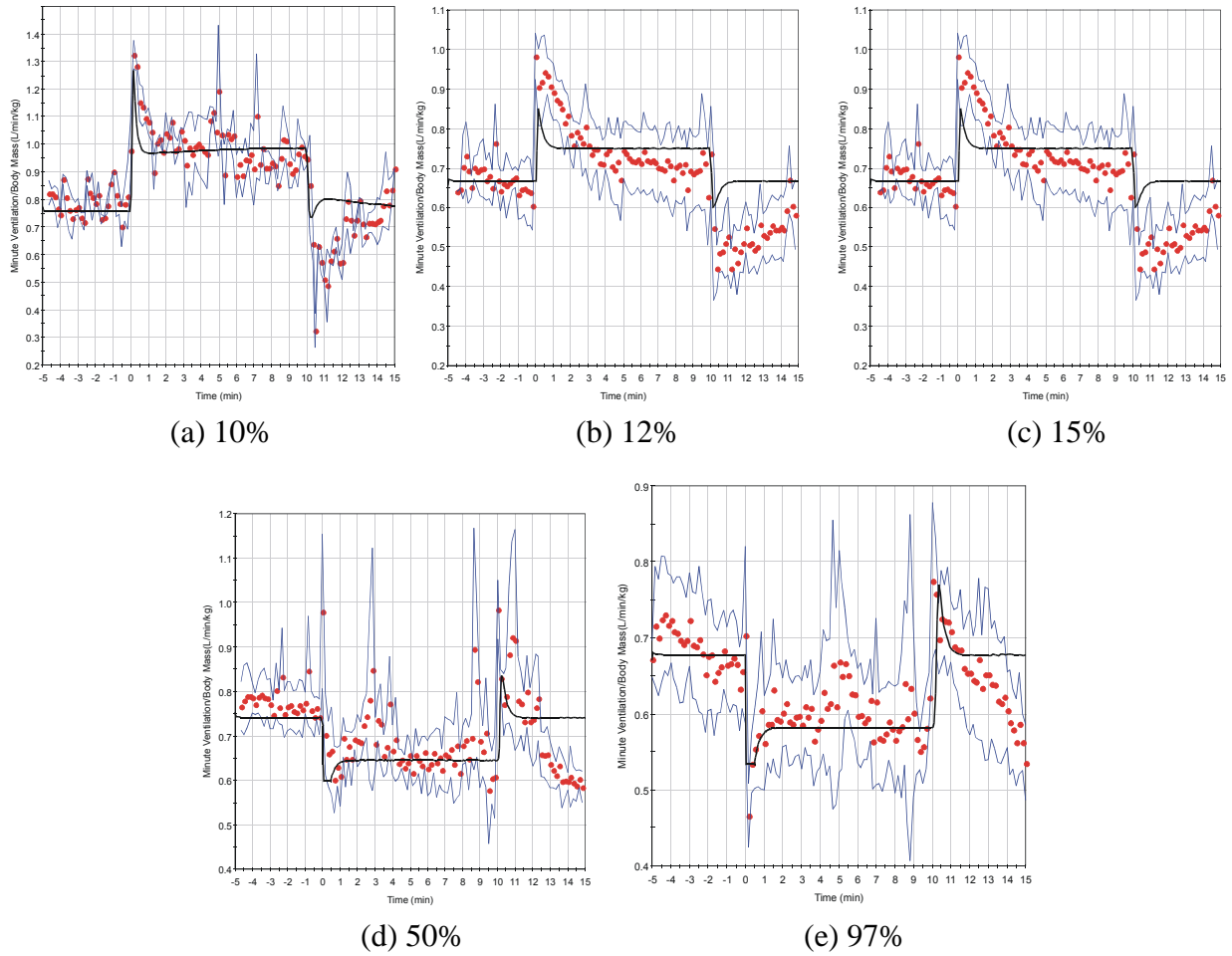


Figure 18. Normalized ventilatory response of rat to a 10-minute exposure to oxygen.

Data from Gu [Gu, Januszkiewicz et al. 2000; Gu and Januszkiewicz 2002; Gu, Januszkiewicz et al. 2002; Gu, Januszkiewicz et al. 2005] averaged over all test subjects. Symbols: \blacklozenge , 10-second averaged minute ventilation normalized by average minute ventilation during pre-exposure period; thin lines, bands of \pm standard deviation of individual averages; thick lines, model simulation.

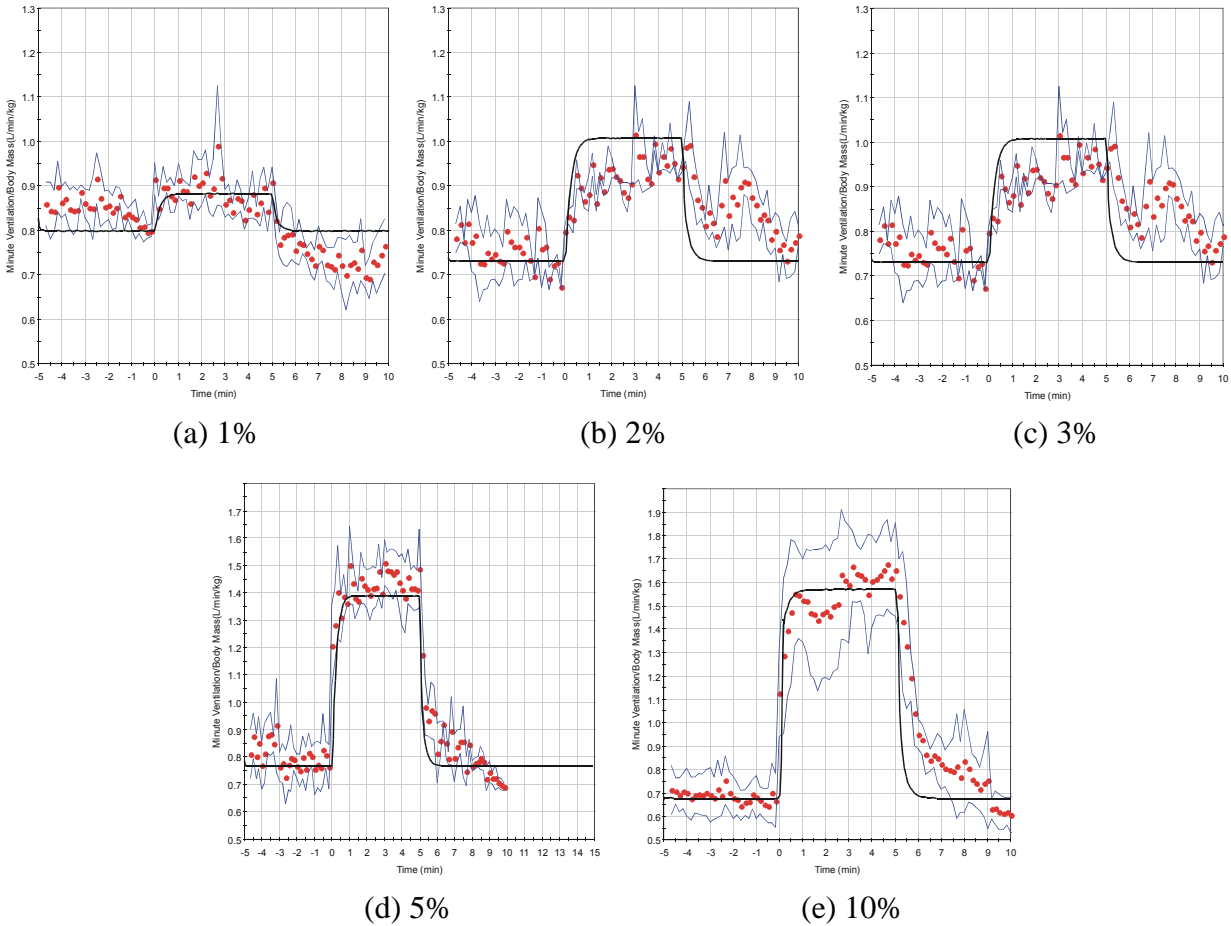


Figure 19. Normalized ventilatory response of rat to a 5-minute exposure carbon dioxide.

Data from Gu [Gu, Januszkiewicz et al. 2000; Gu and Januszkiewicz 2002; Gu, Januszkiewicz et al. 2002; Gu, Januszkiewicz et al. 2005] averaged over all test subjects. Symbols: \blacklozenge , 10-second averaged minute ventilation normalized by average minute ventilation during pre-exposure period; thin lines, bands of \pm standard deviation of individual averages; thick lines, model simulation.

Product 15. Stuhmiller, J.H., Long, D. W., and Stuhmiller, L.M. (2010). Model of acute ventilation changes from inhaled gases—oxygen, carbon dioxide, and carbon monoxide (*in preparation*).

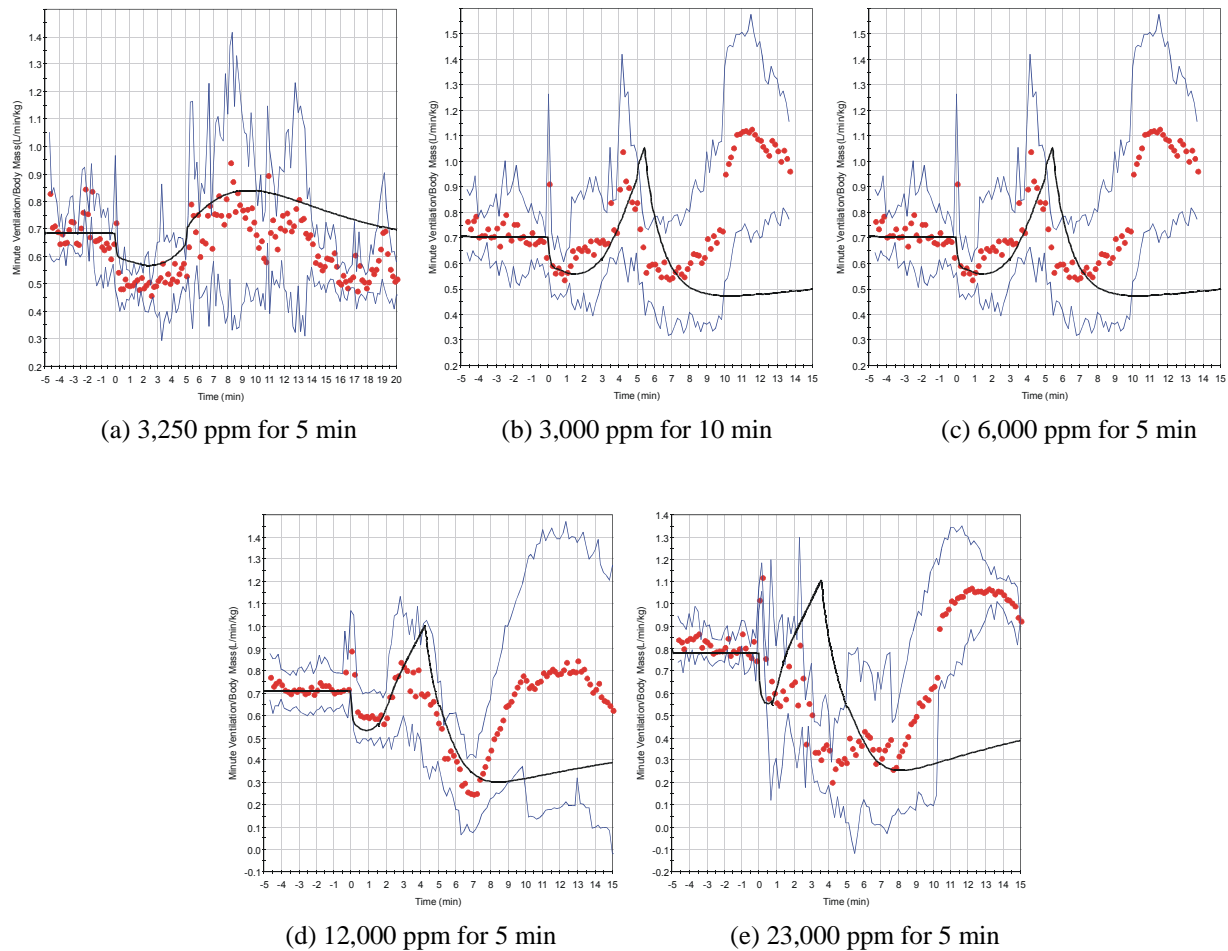


Figure 20. Normalized ventilatory response of rat exposed carbon monoxide.

Data from Gu [Gu, Januszkiewicz et al. 2000; Gu and Januszkiewicz 2002; Gu, Januszkiewicz et al. 2002; Gu, Januszkiewicz et al. 2005] averaged over all test subjects. Symbols: \blacklozenge , 10-second averaged minute ventilation normalized by average minute ventilation during pre-exposure period; thin lines, bands of \pm standard deviation of individual averages; thick lines, model simulation.

2.2 ADVANCED BLAST TEST DEVICE (ABTD)

2.2.1 Development of Advanced Blast Test Device (ABTD)

A rugged version of the Advanced Blast Test Device (ABTD) has been designed to withstand strong blast environments for survivability tests that can also be used for body armor testing. Provided by NSRDEC, the human form dataset used represents mid-size US Army male personnel (Figure 21). Anthropomorphic in shape, the ABTD spans from the neck down to the lower abdomen, and full size body armor can be put on for blast testing. To withstand strong blasts, the device is to be cast from high-strength aluminum.

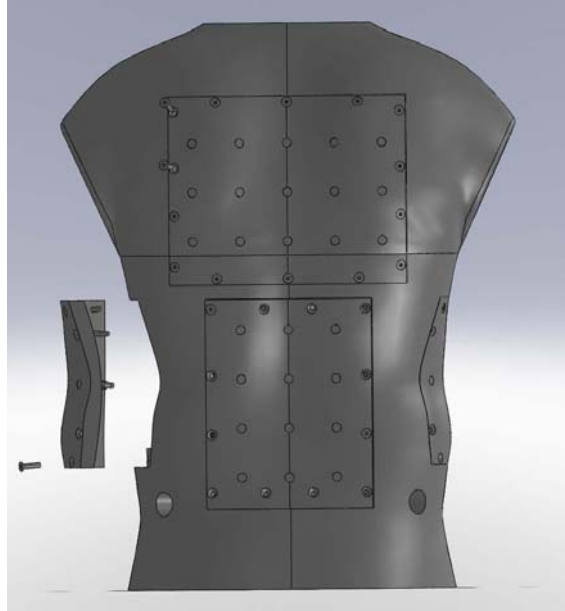


Figure 21. ABTD front view.

The ABTD is designed to be equipped with modular, removable sensor panels on all four sides. For standard blast overpressure testing, distributed pressure sensors will be mounted on the panels to measure pressure loading distribution with or without armor (Figure 22). Internal space is available to accommodate an onboard data acquisition system (DAS).

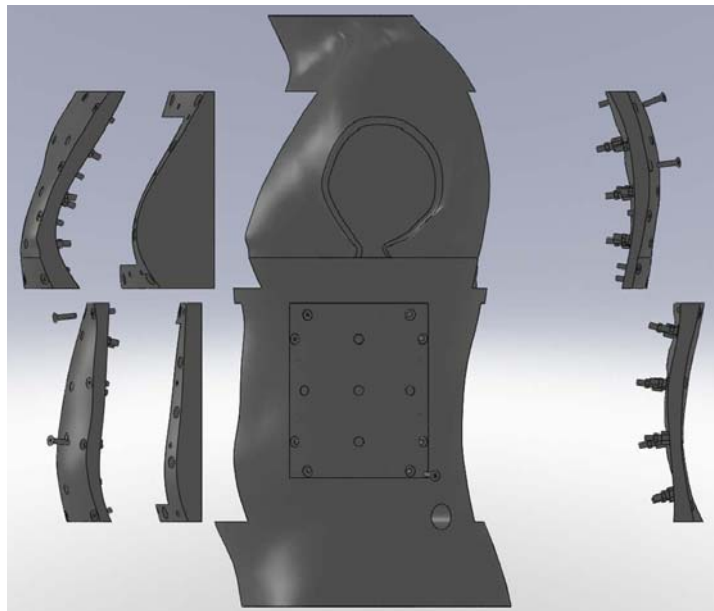


Figure 22. ABTD side view. Modular sensor panels shown.

The ABTD is also designed to serve as an integrated blast test platform to collect data for multimode injury assessments from the same test at the same location. The range of injury modes includes blast lung injury, burn injury, ocular injury, toxic gas injury and ear injury, etc. The sensor panels can be mounted with heat flux sensors and toxic gas sensors. The neck will have an adaptor for attaching an acoustic headform for auditory measurements or a special headform with optical sensors at the eye locations, heat flux sensors on the face and pressure transducers at the ear drum locations. The advantage of having an integrated platform is that multimode data can be collected self-consistently from the same test without running repeat tests with different instrumentation. The ABTD will be constructed in early 2010, followed by field blast testing.

Product 16. Advanced Blast Test Device (ABTD).
--

2.3 HEAD INJURY

2.3.1 ECE Motorcycle Helmet Standard Evaluation (NHTSA Agreement)

Drop tests and finite element model simulations were performed to evaluate the biofidelity of the European ECE motorcycle helmet criteria. Different from the US DOT criteria FMVSS 218, which uses a guided vertical drop with a half-face headform instrumented with a uniaxial accelerometer, ECE uses a free drop procedure with a full face headform instrumented with a triaxial accelerometer (Figure 23). ECE allows the helmeted headform to respond freely upon impact. ECE drops at a slight higher velocity of 7.5 m/s. Twenty helmets were tested, each dropped at the front, side, back and crown locations, half the drops were on the curbed and flat anvils, respectively, producing a total of almost 80 usable data points (Figure 24). For each drop, 36 FlexiForce sensors were mounted on the headform to measure the pressure distribution time traces. The ECE injury limits are the headform resultant acceleration must not exceed 275 g and HIC must not exceed 2400. These limits were evaluated against the validated Skull Fracture Correlate (SFC) developed by Jaycor and the SIMon model-based injury criteria developed by NHTSA.

Data comparison shows that ECE significantly underpredicts skull fracture, where its current thresholds will allow very high likelihood of skull fracture (Figure 23). To keep skull fracture below 15% probability, the headform acceleration and HIC thresholds should be reduced to 185 g and 1600, respectively (Figure 24). Using the headform acceleration as inputs to the SIMon model, results show that the current ECE thresholds are also too high for diffuse axonal injury (DAI). The overall findings show that the biofidelity of the ECE criteria is weak and revisions are needed, similar to the previous findings for the US FMVSS 218 standards previously investigated.

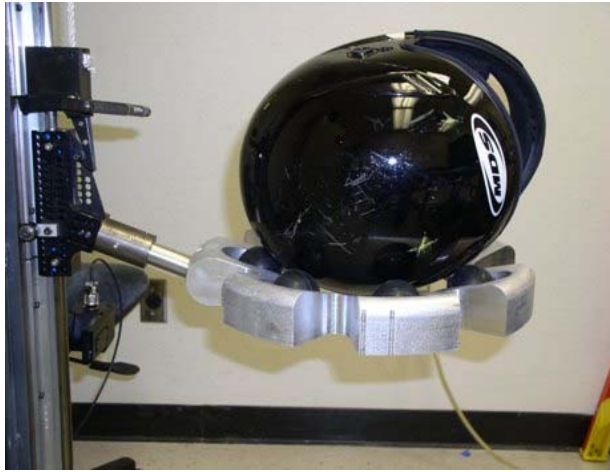


Figure 23. ECE free drop fixture.

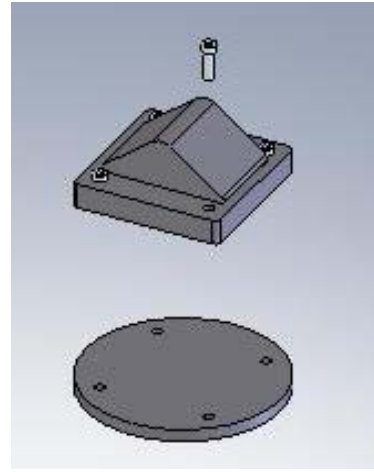


Figure 24. ECE anvils.

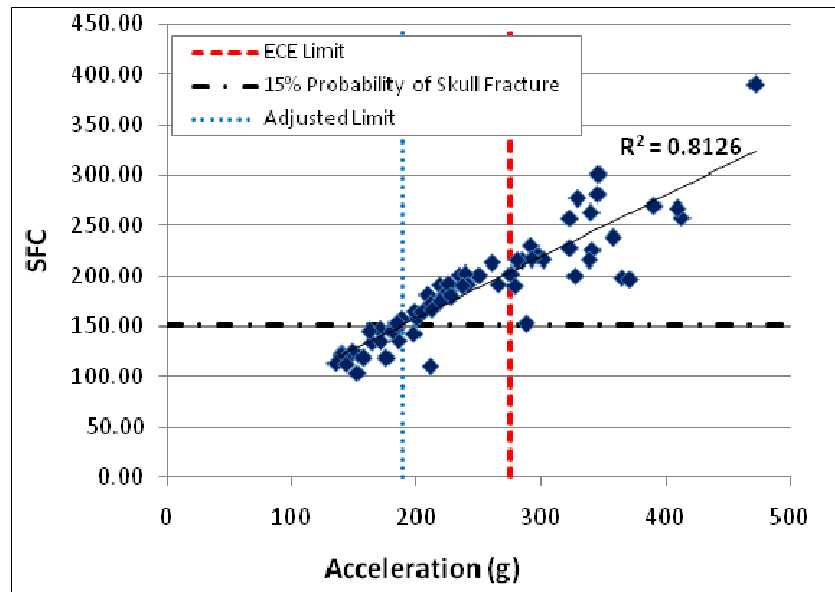


Figure 25. ECE skull fracture comparison with acceleration.

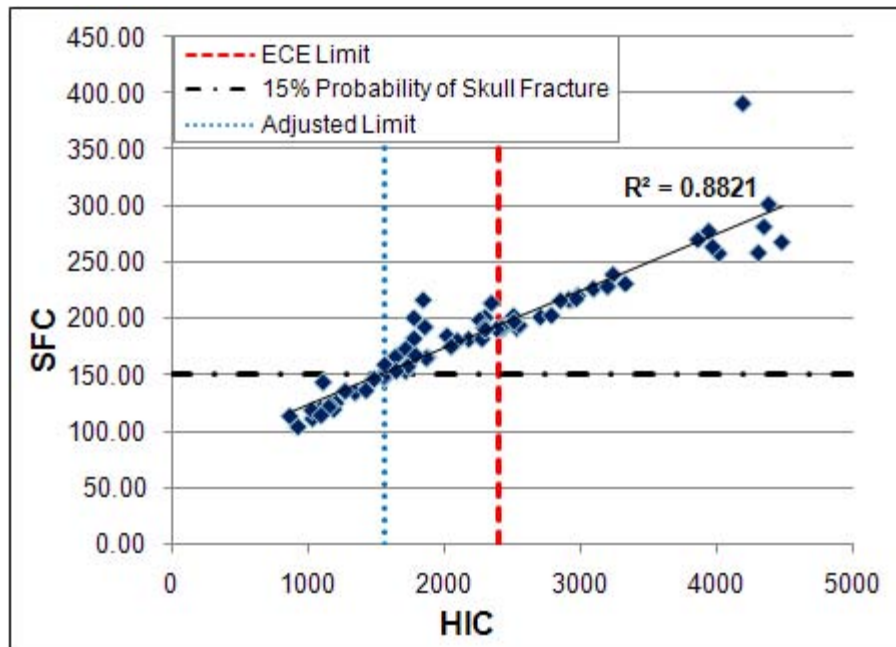


Figure 26. ECE skull fracture comparison with HIC.

Product 17. Rigby, P, Chan, P. (2009). "Evaluation of the Biofidelity of FMVSS No. 218 Injury Criteria," Traffic Injury Prevention, 10:170-188.

2.4 HELMET MOUNTED SENSOR SYSTEMS

2.4.1 Finite Element Model (FEM) – Forward Modeling

Work has been done to refine and expand the capabilities of the current L-3/Jaycor helmeted head finite element model (FEM). The FEM was constructed using the LS-DYNA software for the Advanced Combat Helmet (ACH) with Team Wendy pads. The helmet is modeled as elastic composite materials. The pads are modeled as nonlinear viscoelastic materials with energy dissipation. The helmet and pads are fitted on rigid headforms (Figure 27). The FEM has been used to model a wide range of biomechanical interactions between the helmet and the headform tested in the laboratory. These impacts include shock wave impacts, impacts from drops, pendulum hits and air gun projectile impacts.

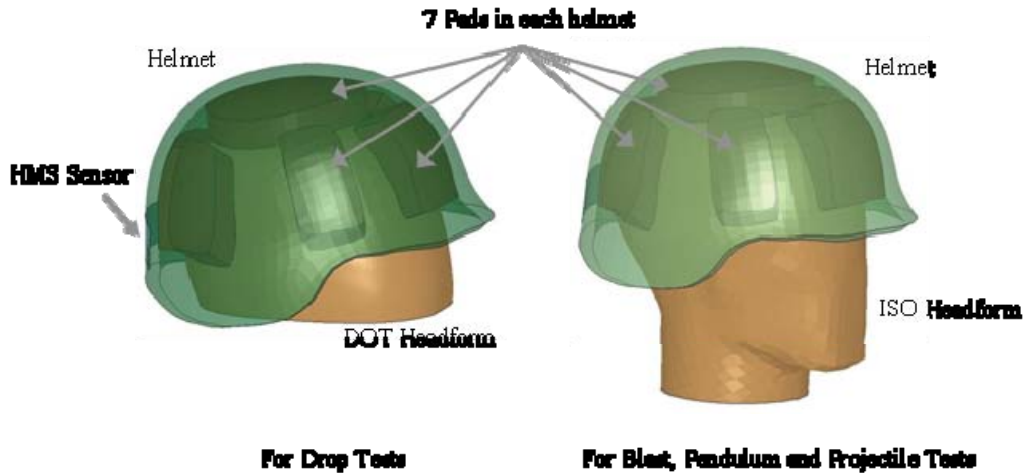


Figure 27. Finite element model of helmet and headforms.

Forward modeling is used to validate the FEM so it can be confidently used to predict the kinematic behavior of the head using the helmet mounted sensors. Forward analysis is done by modeling exact test conditions. A drop test is modeled by prescribing an impact velocity and a rigid impact surface; a blast test is modeled by prescribing the pressure loading to the helmet; a pendulum test is modeled by striking the helmet with a large mass; and the helmet is impacted with a smaller, high velocity mass in the air gun projectile test.

The FEM has been able to predict the head acceleration very closely to the headform acceleration measured in the laboratory in most cases (Figure 28). Injury metrics (average head acceleration and peak head velocity) was calculated from each experimental and corresponding FEM run. The correlation between experimental and predicted average head accelerations is shown in Figure 29. The R2 value of 0.79 demonstrates that the FEM is a valid tool to predict average head accelerations.

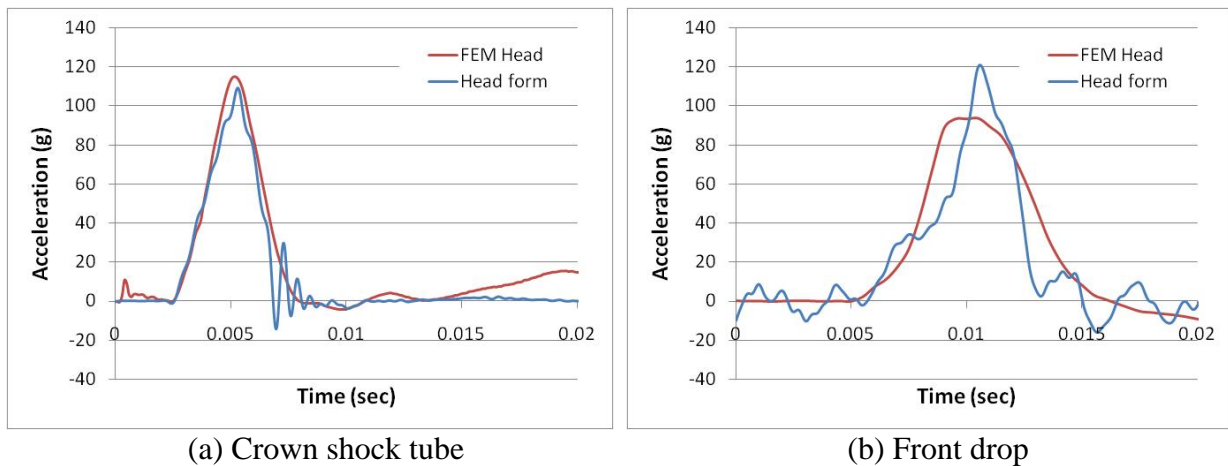


Figure 28. Forward modeling analysis.

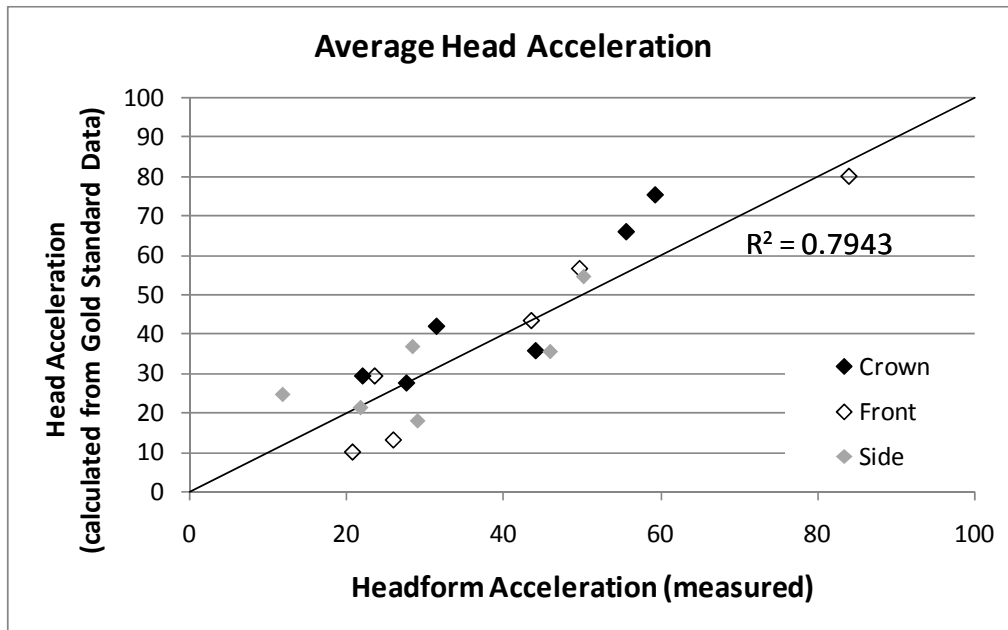


Figure 29. Accuracy of FEM prediction.

2.4.2 Finite Element Model (FEM) – Reconstruction

A finite element model of the helmet-pad-head interaction, built on research for ONR and NHTSA, was used to transfer the helmet dynamics, measured by helmet mounted sensors, to estimates of head dynamics. The accuracy of this mode-based transfer function was tested using helmet dynamics data collected from two high fidelity laboratory accelerometers located at two locations (“front” and “back”) of the helmet. This part of the FEM development was called reconstruction because the impact events recorded by the helmet sensors were used to reconstruct the impact using the FEM. The accuracy of the model was judged by how well the average head acceleration and the head velocity changes are predicted. If laboratory grade sensors were used on the helmet, the FEM was able to predict the resulting head motion with confidence ($R^2 = 0.7987$).

The external HMSS acceleration sensors consistently suffer a shift in the zero level following the initial phase of impact that causes the acceleration data to be consistently under predicted. This effect is most clearly seen in the helmet velocity (integral of the acceleration) in the direction of impact. The velocity rises more slowly than the true velocity and then decays at a constant rate (Figure 30). An algorithm has been developed to apply a step increase in the measured acceleration that counteracts the offset caused by impact. Nearly every external HMSS record collected during laboratory testing could be adjusted in this manner. The internal HMSS device

shows a similar pattern of artifact in about half the cases; the other half produce acceleration traces that are not correctable.

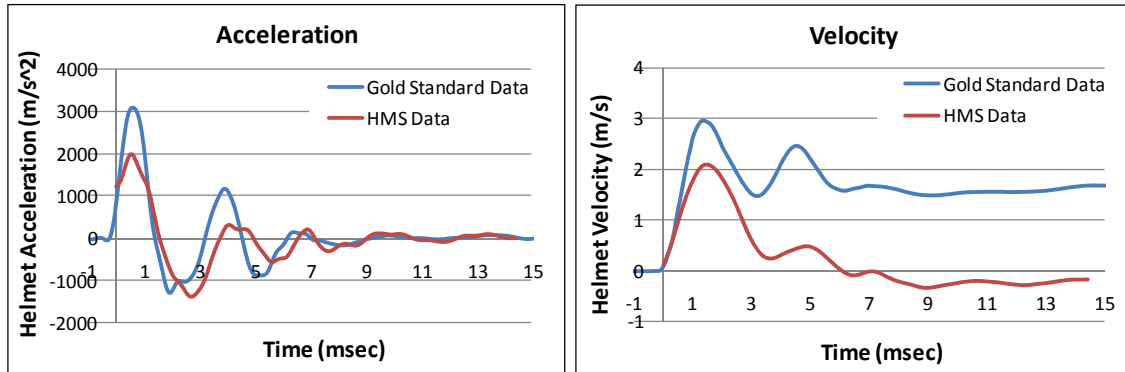


Figure 30. Offset seen in external HMSS sensors.

The fielded HMSS devices record the helmet acceleration at a single location; however, laboratory data have shown that the helmet has both linear and angular motion during impact and that both are required to estimate accurate head acceleration. A correlation between motion at the front of the helmet to that to the back of the helmet was observed and used when reconstructing field sensor impact events. The acceleration offset correction and the estimate for total helmet motion constitute the “correction” algorithms used to make HMSS data suitable for analysis by the model-based transfer function.

The external HMSS device produced usable data in virtually every laboratory test condition (drop, blast, pendulum impact) and at every direction (crown, front, side), and intensity (high, medium, low). The accuracy of the prediction of head injury dose is shown in the following figures (Figure 31). As expected, the accuracy is less than what can be achieved with laboratory sensors, but still adequate for injury screening purposes. The internal HMSS device produced usable data in about half of the test conditions, but for those conditions the accuracy in both magnitude and rank order were quite acceptable (Figure 32).

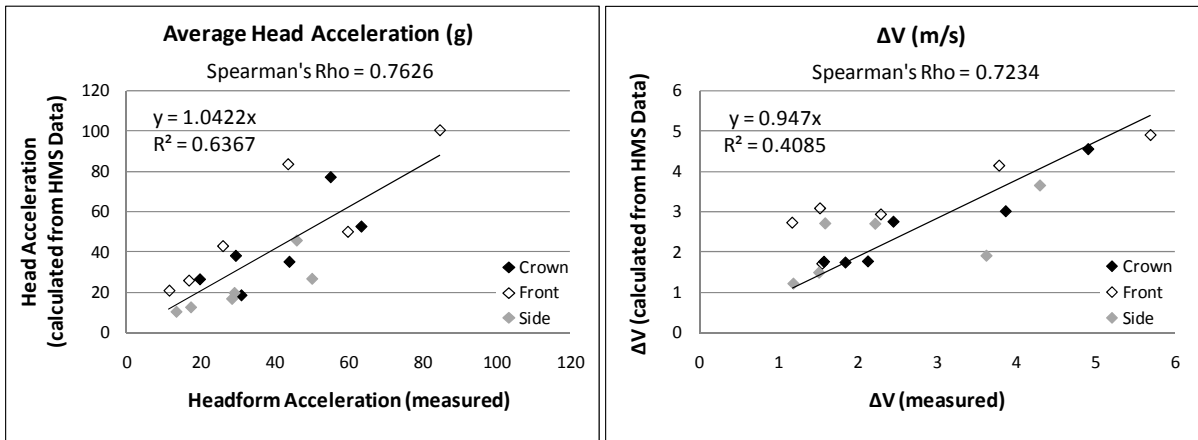


Figure 31. Calculated head injury metrics using external mounted sensor

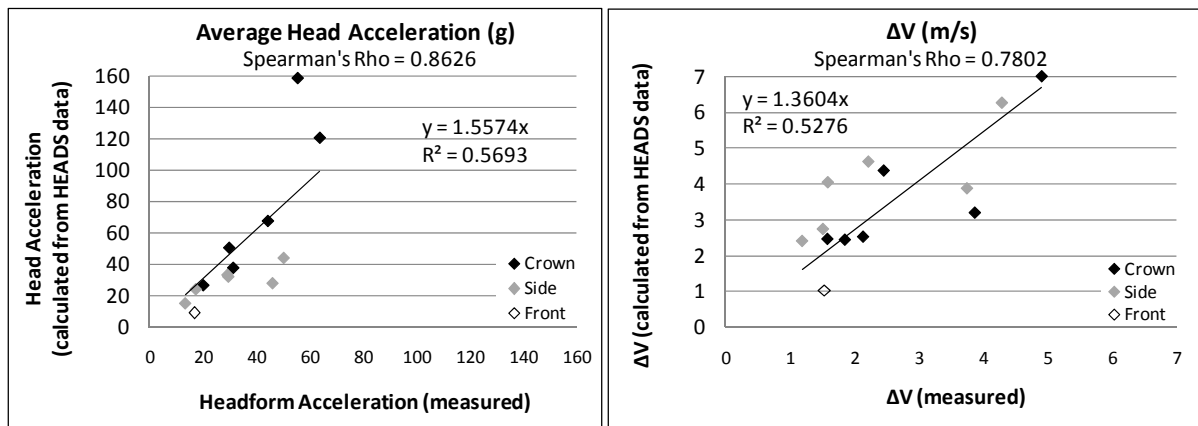


Figure 32. Calculated head injury metrics using internal mounted sensor

2.4.3 Testing

The goal of the helmet impact testing was to create a knowledge base of how the helmet / head combo react to various types of impacts. The baseline data were then used to help design and validate the helmeted head finite element model, quantitatively evaluate the performance of the fielded helmet sensors system, and help develop guidelines to screen out garbage signals from the database of field data. A battery of laboratory impact tests have been conducted using high fidelity (“gold standard”) instrumentation to completely define the external loading, helmet acceleration, and head acceleration for a wide range of possible impact events. These experiments have also been conducted with the internal and external helmet mounted sensors mounted on the helmet.

The tests conducted were shock tube blast tests, drop tower impact attenuation tests, pendulum impact tests, air gun projectile impact test, and ballistic impact tests (Figure 33). When possible for each test, the helmet was impacted on the crown, front and side. Each impact was repeated three times with the pads replaced for each test. Example plots show that the helmet acceleration is completely different from the head acceleration—it occurs at different times, with different magnitudes, and different durations (Figure 34, Figure 35). It is clear that the relation between them must be described by a model of this complex dynamics.

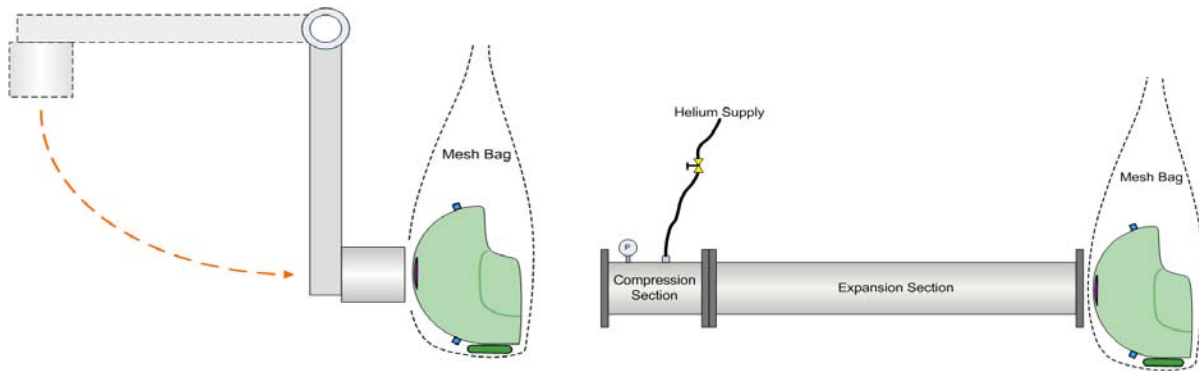


Figure 33. Sample setup for a pendulum and shock tube impact

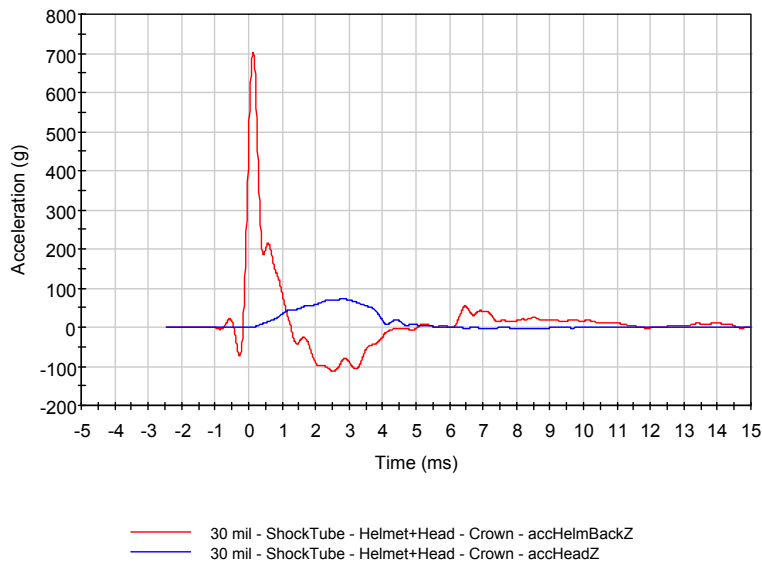


Figure 34. Helmet and head acceleration – shock tube

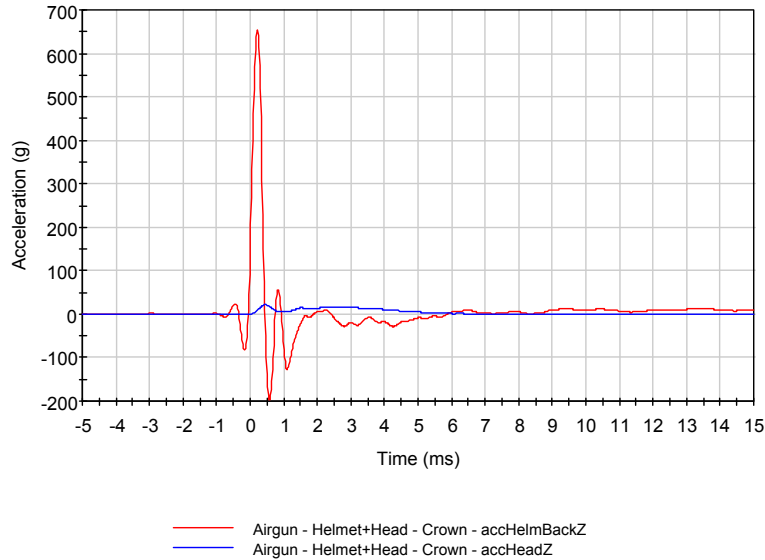
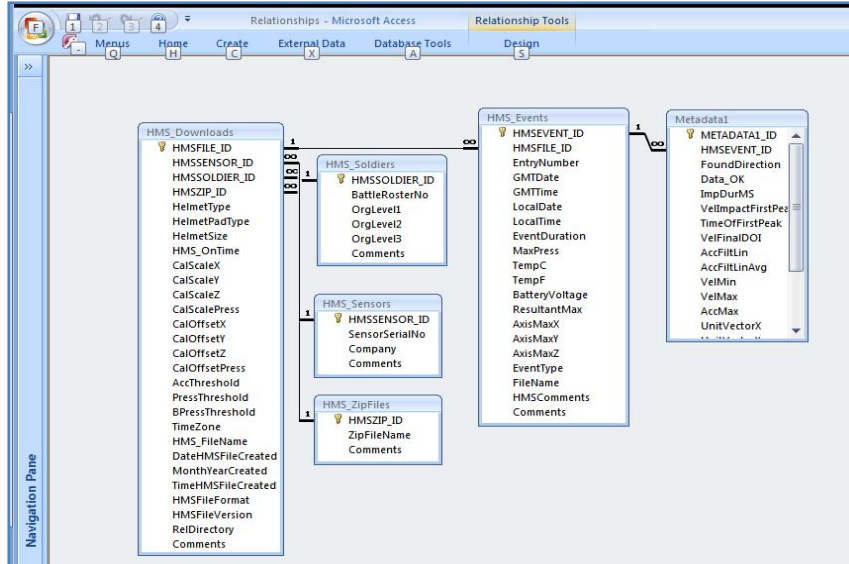


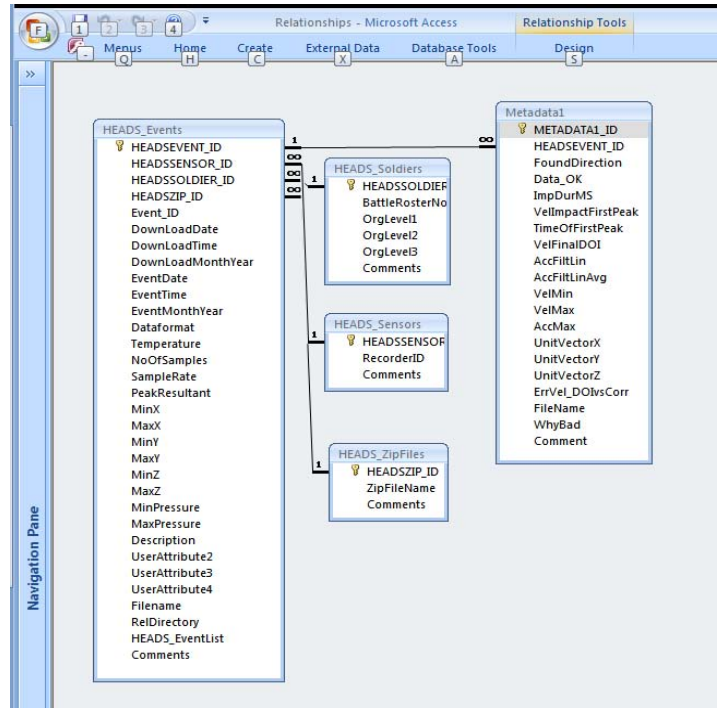
Figure 35. Helmet and head acceleration – air gun projectile

2.4.4 HMSS Field Data Organization

Two data sensors were deployed in the field for the HMSS project: an external (HMS) sensor and an internal (HEADS) sensor. The raw data was received from both types of sensors and the HMS and HEADS data information were added to the HMS_FieldData database and the HEADS_FieldData database, respectively (Figure 36). The raw data was then copied to the appropriate data directory and converted to GDIF format for further analysis (Figure 37). Two additional databases, HMS_FieldData_Reports and HEADS_FieldData_Reports, were developed to create statistical reports for the data received. The data was then processed further to obtain additional information about the data and these results were stored in a Metadata table in the database and in GDIF files in the directory structures.

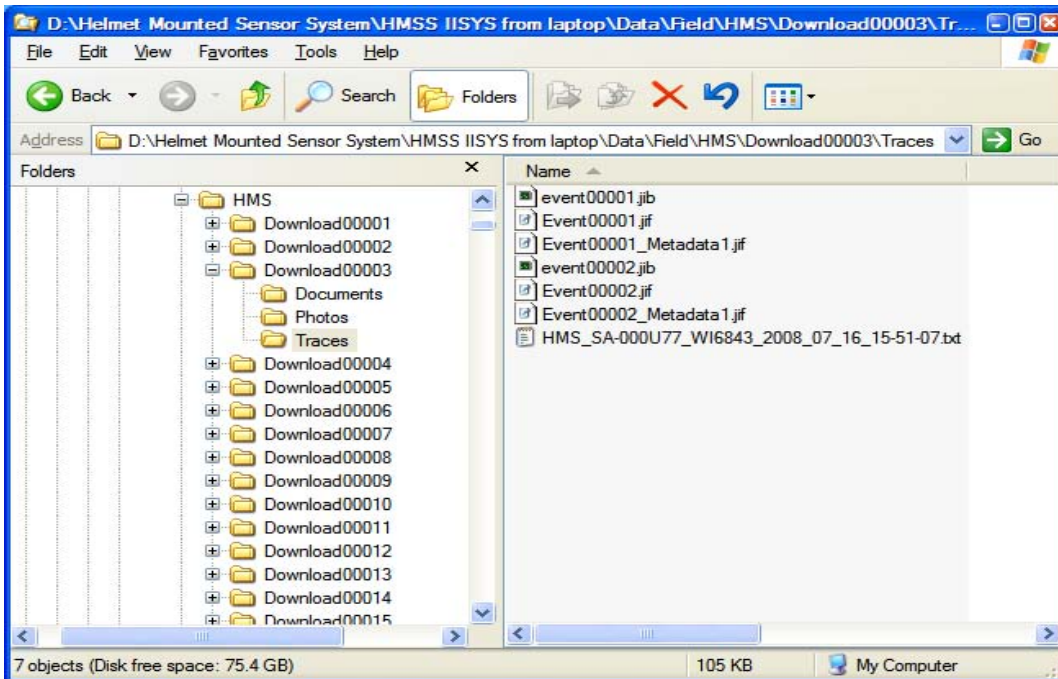


(a) HMS sensor database

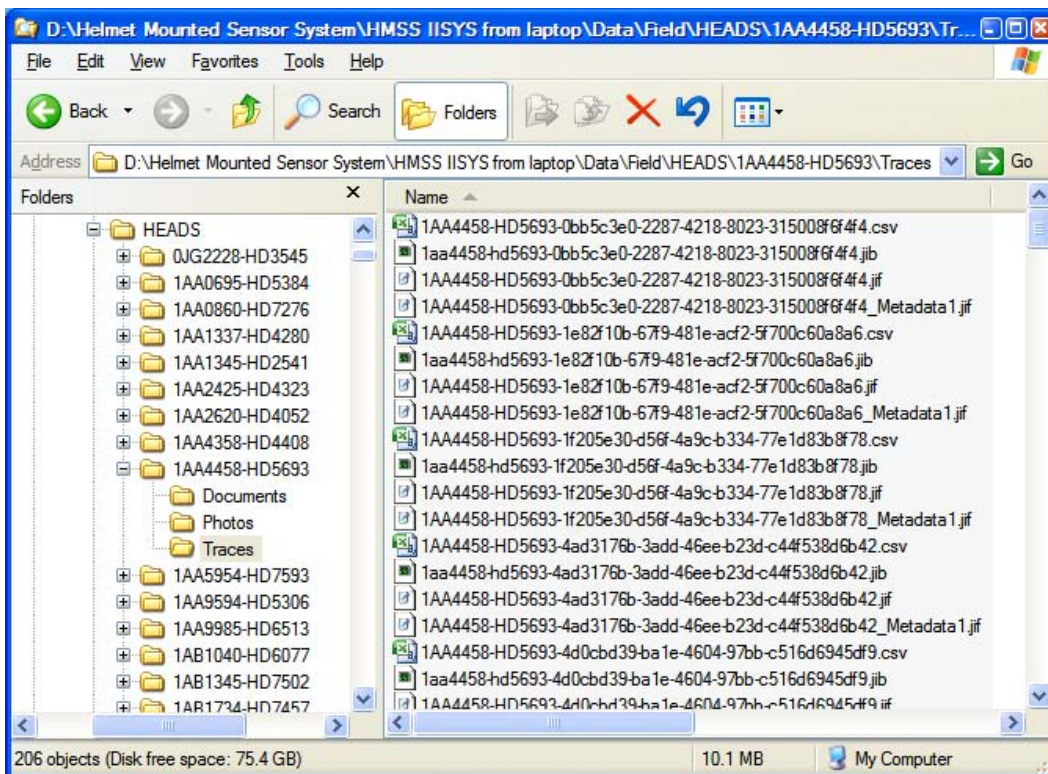


(b) HEADS sensor database.

Figure 36. Relational databases for field data.



(a) HMS data directory



(b) HEADS data directory

Figure 37. Field data directory structure.

- Product 18. Stuhmiller, J. H. Chan, P.C., Chilton, W.E., Dang, X., Long, D.W., Rigby, P.H., Tracy, B.J., Wong, J., and Yang, W. (2009). Technical Support for Combat Helmet Sensor Fielding Project, Vol. 1: Technical, L-3 Communications/Jaycor, San Diego, CA. Midterm Report J0287-09-366, 108 pp., Jan. 2009.
- Product 19. Stuhmiller, J. H. Chan, P.C., Chilton, W.E., Dang, X., Long, D.W., Rigby, P.H., Tracy, B.J., Wong, J., and Yang, W. (2009). Technical Support for Combat Helmet Sensor Fielding Project, Vol. 1: Appendices, L-3 Communications/Jaycor, San Diego, CA. Midterm Report J0287-09-366A, 110 pp., Jan. 2009.
- Product 20. Stuhmiller, J. H. Chan, P.C., Chilton, W.E., Dang, X., Long, D.W., Rigby, P.H., Tracy, B.J., Wong, J., and Yang, W. (2009). Technical Support for Combat Helmet Sensor Fielding Project, Vol. 1: Technical, L-3 Communications/Jaycor, San Diego, CA. Annual Report J0287-09-376, 110 pp., Aug. 2009.
- Product 21. Stuhmiller, J. H. Chan, P.C., Chilton, W.E., Dang, X., Long, D.W., Rigby, P.H., Tracy, B.J., Wong, J., and Yang, W. (2009). Technical Support for Combat Helmet Sensor Fielding Project, Vol. 1: Appendices, L-3 Communications/Jaycor, San Diego, CA. Annual Report J0287-09-376, 138 pp., Aug. 2009.

2.5 BLAST BEHIND ARMOR

2.5.1 INJURY-A Development (NSRDEC ATO)

The INJURY-A model has been developed to calculate normalized work with armor coupling to the chest wall motion (Figure 38). Using BTD and MBTD data, a method has been developed to derive armor material models as tested (Figure 39). From field tests, the average under-armor pressure on each quadrant of the MBTD is obtained from the 9 pressure sensor data traces. The matching BTD data without armor represent the pressure loading on top of the armor. Applying Newton's Second Law to the armor material for each MBTD quadrant, the force vs. displacement curve for the material response (model) can be obtained after double integration of the material acceleration. The material model is then used for coupling the armor to the chest wall motion to calculate normalized work using INJURY 8.2. Using this method, the material response model is calculated specifically for each quadrant of the MBTD for each test condition.

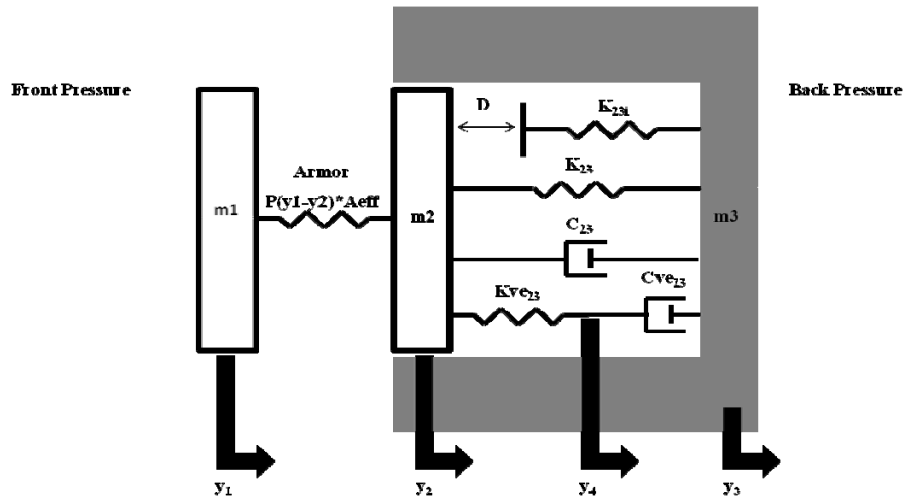


Figure 38. INJURY-A schematics.

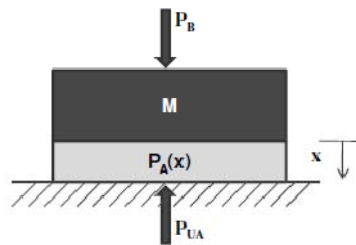


Figure 39. Force balance on armor material.

Calculations were performed for the Blossom Point tests with good data agreement with the animal lethality outcomes. A sensitivity study was also carried out using shock tube test data to derive the material model at comparable pressure levels as the field tests, which also produces good data agreement (Figure 40). This shows that shock tube tests can be used cost effectively together with INJURY-A to screen material concepts. INJURY-A will be packaged as software.

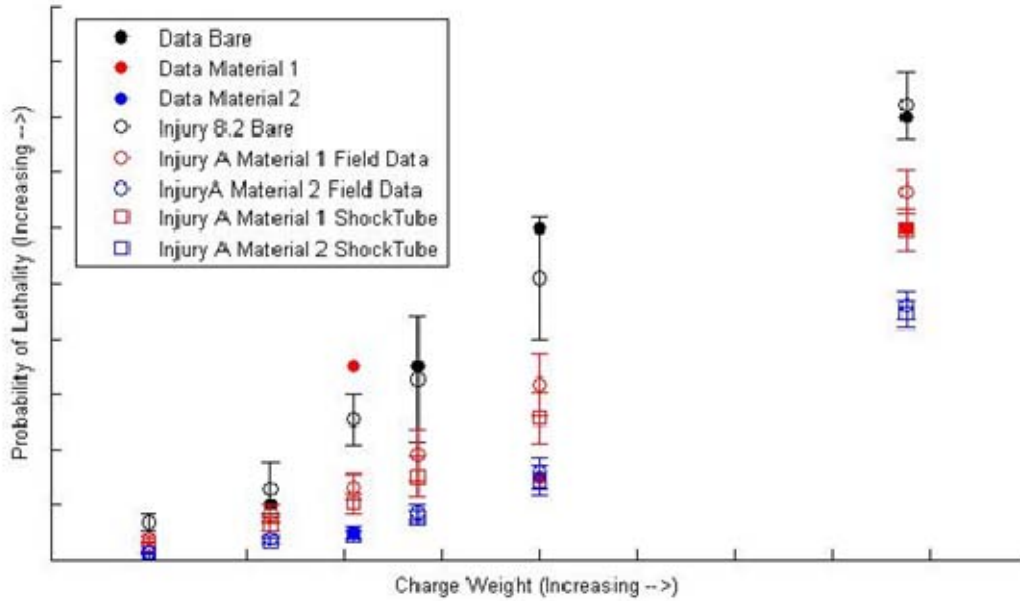


Figure 40. INJURY-A data comparison.

Product 22. P. Chan, MacFadden, L., Dang, X., Ho, K., Maffeo, M., Carboni, M., and DeCristofano, B. (2010). “Study of Material Effects on Blast Lung Injury using Normalized Work Method,” accepted for presentation at PASS2010, Quebec, Canada, September 2010.

Product 23. INJURY-A – A model for predicting blast injury with armor effects.

2.5.2 MBTD Tests and Data Screening Software (NSRDEC ATO)

A new series of MBTD tests was conducted at Blossom Point to replace previous data corrupted by electrical problems at the field. The MBTD was equipped with 36 sensors (9 per panel) (Figure 41). A wide range of armor materials was tested with under-armor pressure distribution measured (Figure 42). Multiple repeat shots were conducted at matching conditions with the previous animal tests.

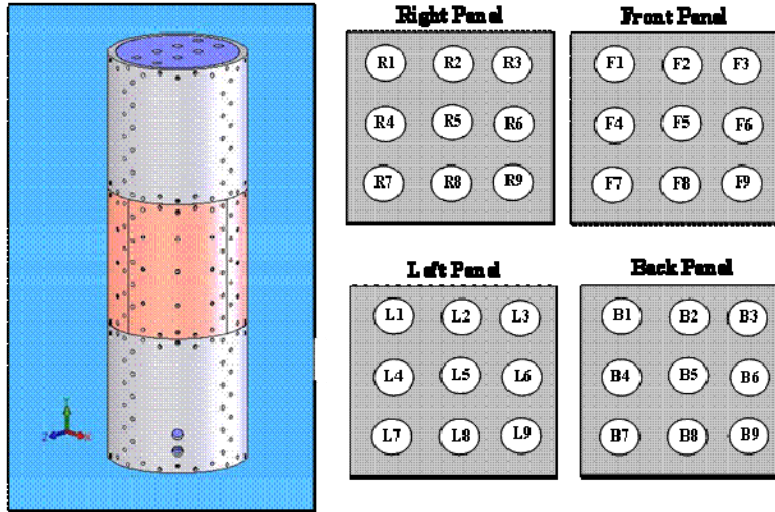


Figure 41. MBTD and sensor schematics.



Figure 42. MBTD with armor.

A data screening algorithm was developed to screen out bad pressure traces (Figure 43). Since data from multiple shots were collected (which is usually the case in field tests), statistical mean and standard deviation values were calculated for each test. Data traces were screened by identifying the outliers for peak pressure, impulse and normalized work following a procedure. Verified by field data analysis, the algorithm was packaged as software with a Graphical User Interface for NSRDEC.

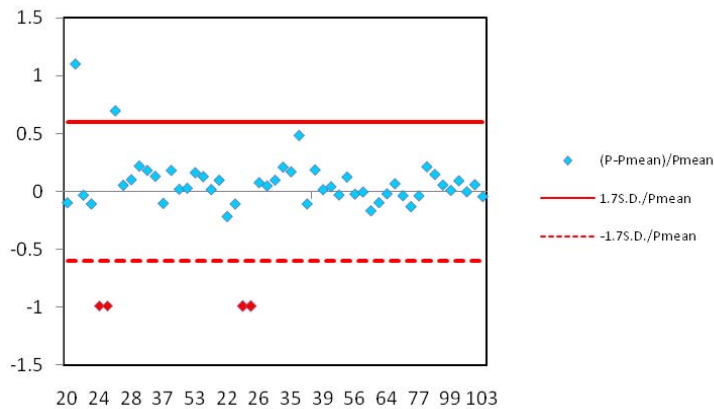


Figure 43. Screening of data outliers.

Product 24. Whang, C., Ho, K., Long, D., and Chan, P. (2009) “MBTD Data Analysis Algorithm and Software,” Technical Report J0287-09-368 for Contract W81XWH-06-C-0051, CLIN0002” prepared for NSRDEC.

Product 25. MBTD data screening software.

2.5.3 Sheep Blast Test Device (SBTD) Tests (NSRDEC ATO)

The Sheep Blast Test Device (SBTD) was developed for field testing to collect blast over-pressure data on the four sides of the thorax for comparison with the BTM (Figure 44). Cast from high-strength aluminum, the SBTD geometry was based on the CT-scan image data from a 100-lb sheep similar to one tested in the field. Two ways of sensor mounting were also tested for the SBTD, one with the sensor canted to flush with the thorax surface, and another mounted horizontally like that for the BTM. Field tests were conducted over a range of charge levels to collect matching data between the SBTD and BTM at Blossom Point. No armor material was used. Normalized work values were calculated using INJURY 8.1.



Figure 44. Sheep Blast Test Device.

Field test analysis shows the BTBD produces essentially the same results as the SBTD. No significant differences were found between the pressure traces recorded by the BTBD and the SBTD, with canted or horizontal sensor mounting (Figure 45). Consequently, the normalized work values were practically the same between the SBTD and BTBD for matching tests. Findings affirm the advantage of using the omni-directional BTBD for nonarmored tests where one data set can be used for predictions of injuries for all four orientations relative to the blast.

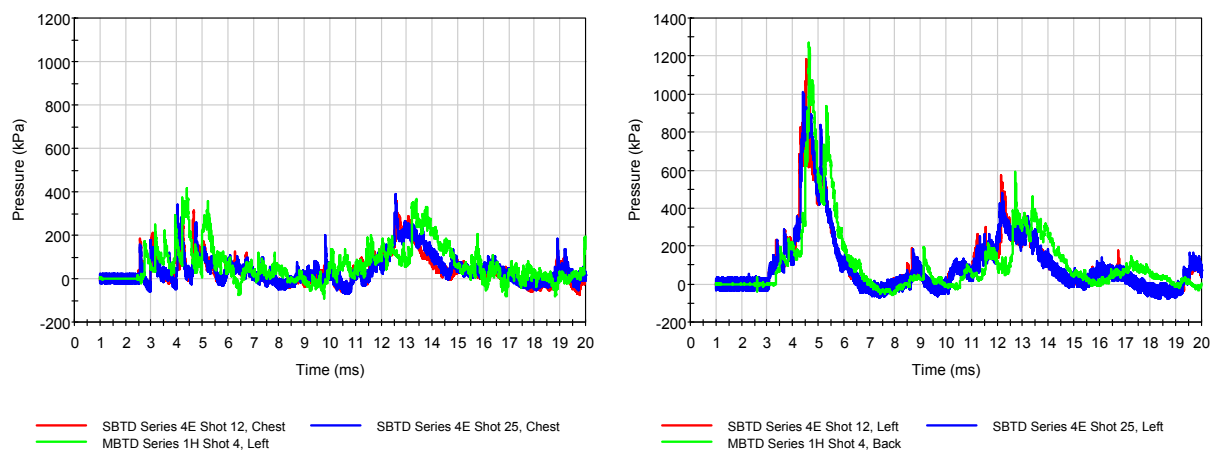


Figure 45. Test results showing no significant differences in pressure data from SBTD and BTBD.

Product 26. Sheep Blast Test Device (SBTD).

2.5.4 Sheep Tests and FEM Development (NSRDEC ATO)

To support the development of the sheep finite element model (FEM) for blast injury studies, a series of sheep thorax dynamic compression tests was carried out using sheep carcasses at Medical College of Wisconsin (MCW) under approved protocol (Figure 46). The tests were performed using a compression piston with well-controlled loading rates and displacement limits using two test subjects. The thorax compression data are being used for model validation (Figure 47). CT-scan image data were obtained for each sheep subject before and after testing for finite element model meshing. Post-test necropsy was also performed for each sheep subject after testing. Rib specimens were preserved for three-point bending, compression and coupon tension tests to derive material properties.



Figure 46. Frontal compression test.

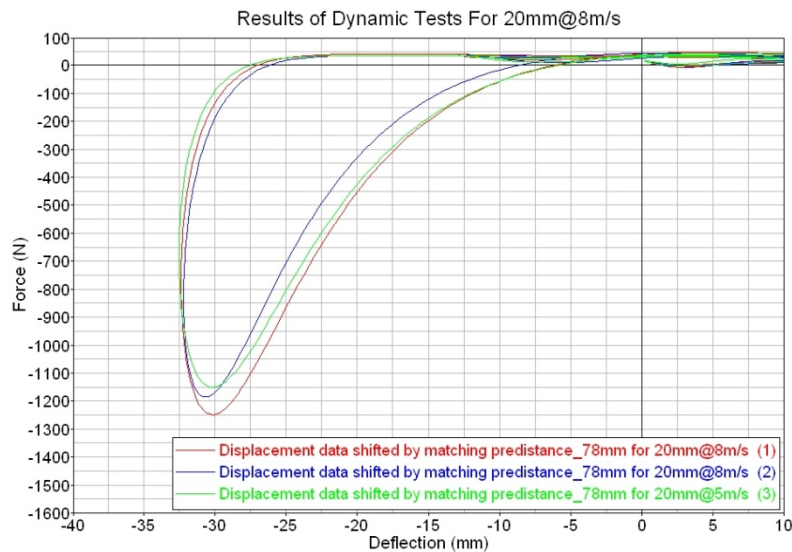


Figure 47. Frontal compression data at 8m/s.

Thorax compression tests were carried out at 3, 5 and 8 m/s loading rates. One subject was tested under lateral (left-right) compression, and one for chest (front-back) compression. To assure the compression tests would be carried out within the noninjurious range, a displacement

limit was first established using very slow (quasistatic) compression rate for each compression direction. Dynamic test data show a rate-dependent, viscoelastic and energy dissipative nature of the thorax, and the thorax is stiffer with a lower threshold of ribcage injury in the front-back direction than the lateral. Overall, fairly repeatable data were obtained for each compression rate.

A series of rib specimen test data were also obtained using three-point bending, compression and coupon tension tests for material model construction (Figure 48). Data show the rib material properties are nonlinear. The rib material property data are being used in the finite element model.

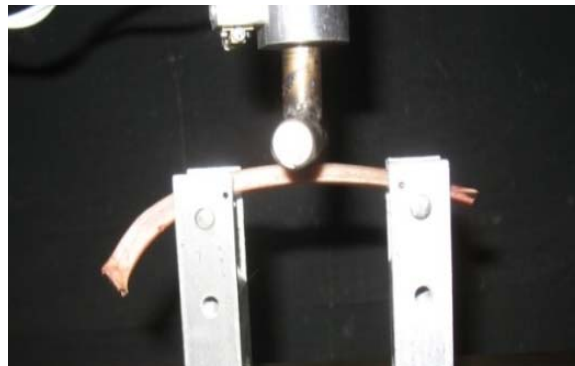


Figure 48. Three-point rib bending test.

2.6 BEHIND ARMOR BLUNT TRAUMA

2.6.1 Blunt Trauma Assessment Tools

FY09 blunt trauma assessment tools research focused on developing and validating computer models that are capable of predicting lung injuries due to blunt impact. These models account for the complete pathway from initial damages in parenchyma at impact to the progression of damages resulting in decrements in lung functions (Figure 49).

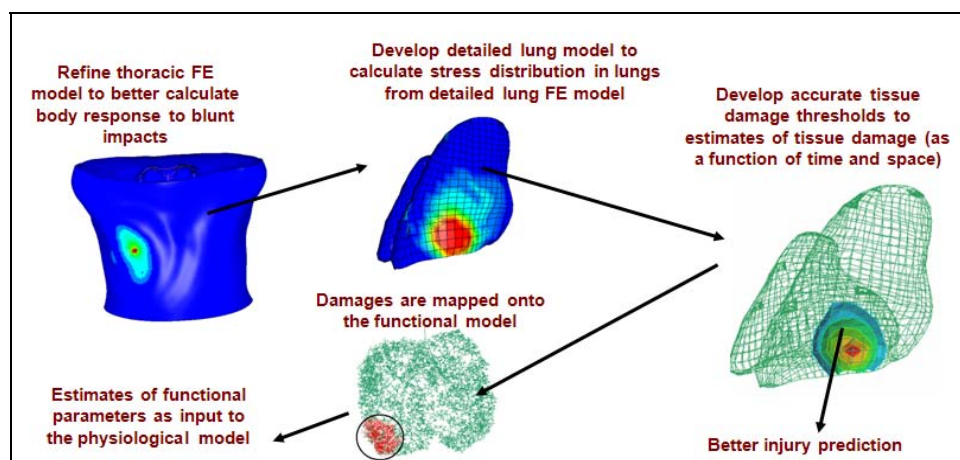


Figure 49. Schematics of the research method to accurately predict lung injuries due to blunt impacts.

The following subtasks were completed during this fiscal year to support the goal.

- **Thorax FEM Improvement.** The current thoracic finite element model, which assumes uniform material distribution, was improved to incorporate the detailed anatomical model of the lungs (Figure 50). It included the macroscopic model of the lungs and predicted the temporal and spatial stress distribution during the blunt impacts. Both animal and human models were refined with the animal finite element models validated against the measured chest response (motion and force) and the lung pressure measurements.



Figure 50. Detailed finite element model of swine lungs and their incorporation in swine torso.

- **Anatomical and functional modeling of lungs.** The anatomical model included the details of lung anatomy and the morphology of the bronchi and blood vessel abortion structures. Lung anatomy was abstracted and categorized by lobes and regions. The functional model predicted the functional parameters of regions of lungs and the whole lung from the properties of local tissue.
- **More accurate lung injury model.** Advanced image processing algorithms were developed to align the medical images collected before and after impact insults (Figure 51). This allowed the accurate determination of lung injuries, including location and severity of edema and hemorrhage at specified time after insults. Rules of progression of edema were adopted to interpret the time evolution of the damage, which allowed the determination of spatial distribution of tissue damage at impact. Side by side comparison of finite element simulations of animal tests and subsequent lung tissue damages produced better lung tissue damage thresholds than previously estimated.

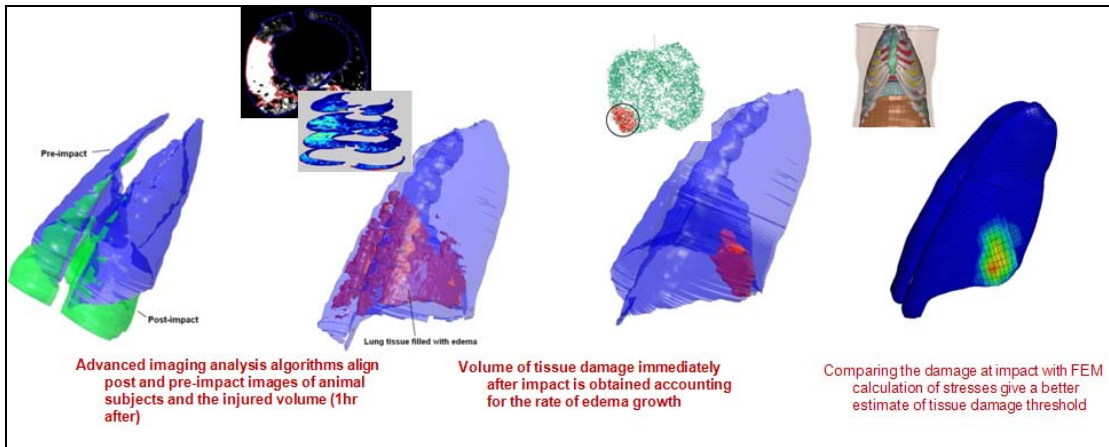


Figure 51. Determine lung tissue damage threshold based on advanced imaging processing, computer simulation and statistical analysis.

In FY09, we also designed the Blunt Trauma Assessment Tools (BTAT) software that provides the general analysis capabilities related to blunt trauma injuries. The high-level design of software has been completed (Figure 52). The actual implementation focused on one specific application module – the assessment of blunt trauma behind armor during ballistic impacts.

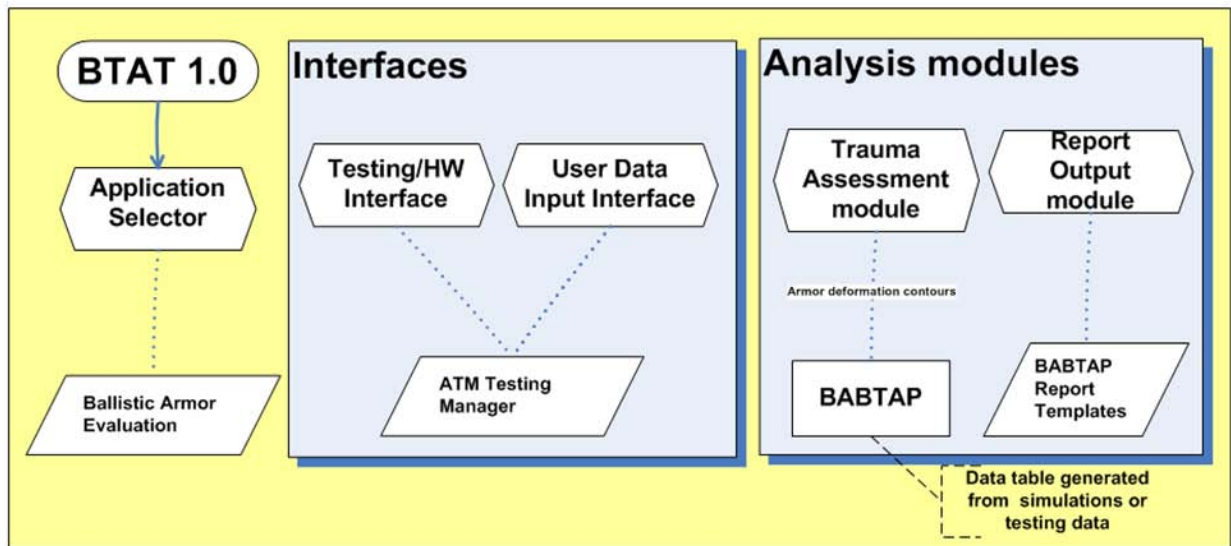


Figure 52. High-level design of BTAT 1.0

Product 27. Human Thoracic Model.

Product 28. Blast Trauma Assessment Tool (BTAT) software.

2.7 ANTHROPOMORPHIC TEST DEVICE EVALUATION

2.7.1 THOR Dummy Air Bag Tests (NHTSA Agreement)

Air bag tests were performed to evaluate the DOT THOR-05F dummy, which is a new anthropomorphic test device with many notable features, including a biofidelic neck design with built-in lordosis that segregates load paths within the cervical spine. Static air bag deployment tests were carried out with the dummy positioned in the NHTSA-1 (chin on module) driver Out-Of-Position (OOP) configuration. A set of late-model two-stage air bag modules were used in a total of forty tests, including reference tests conducted with the 5th percentile female Hybrid III dummy. Half of the modules were configured to deploy more aggressively. The THOR-05F demonstrated its ability to discriminate air bag aggressiveness, especially in its upper neck tension measurements which was the most predominant upper neck load (Figure 53, Figure 54). Compared to Hybrid-III, the THOR-05F neck showed a lower tendency to go into extension. The upper neck moment (M_y) and shear (F_x) were much lower in magnitude than those of the Hybrid III-5th. Head accelerations were similar to those produced by the Hybrid III-5th.

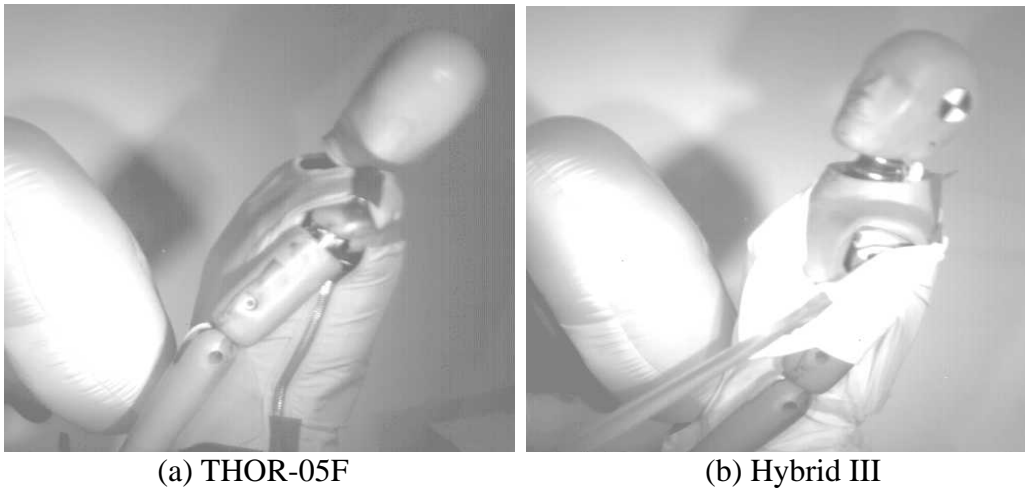


Figure 53. THOR-05F vs. Hybrid III for Aggressive Bag: head position at bag separation.

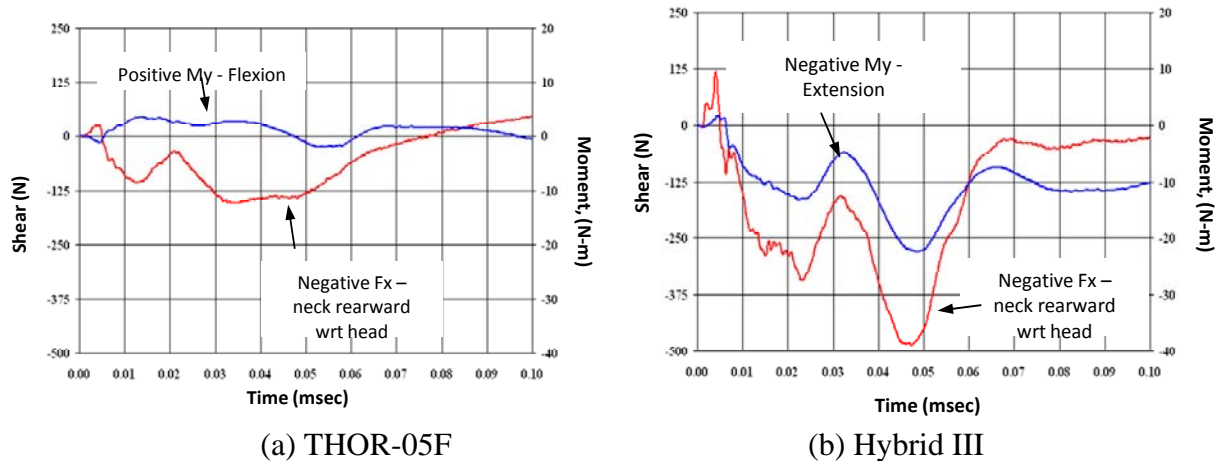


Figure 54. THOR-05F vs. Hybrid III for Aggressive Bag: head position at bag.

Product 29. Martin, P., Craig, M., Ridella, S., Rigby, P., and Chan, P. (2009) "OOP Air Bag Tests using the 5th Percentile Female THOR and Hybrid III Dummies," Paper Number 09-0546, 21st International Technical Conference on the Enhanced Safety of Vehicles Conference (ESV), Stuttgart, Germany, June 15-18, 2009.

2.8 DATA PRESERVATION

2.8.1 Historical Data Recovery and Bowen's Test Data Analysis

Work has continued to recover the historical blast data using the IISYS data management system. Identified test reports were scanned into PDF files and cataloged into an EndNote database. Data traces from strip chart records were cross linked to specific tests and digitized. Injury data from photographs were also digitized and cataloged in IISYS. Work will continue in 2010.

Using the historical data archive, analysis was carried out to support ARL/SLAD in the design of field tests using Blast Test Devices (BTD's) to replicate the Bowen's tests to collect data for normalized work calculations for correlation with Bowen's lethality data (Figure 55, Figure 56). The findings will further refine and generalize the lethality correlation for open and complex blast conditions. Since the original Bowen's tests were conducted at Albuquerque, NM at about 5000 ft elevation, Sach's scaling analysis was performed to determine the equivalent test conditions at sea level where the new tests will be carried out (Figure 57, Figure 58). Scaling calculations were performed by two ways: (1) keeping the standoff the same, which requires higher charge weights; or (2) keeping the charge weights the same, which requires shorter standoff conditions. The calculations were sent to ARL/SLAD and multiple consultation discussions were held.

Point	Charge type	Species	Ambient Pressure (psi)	Charge Weight (lb)	Reflected Pressure (psi)	Scaled Reflected Pressure (P bar)
1	TNT	Dog	12	8	275.00	22.92
2	TNT	Dog	12	8	229.00	19.08
3	TNT	Dog	12	8	122.00	10.17
4	TNT	Dog	12	64	100.00	8.33
5	TNT	Dog	12	64	94.30	7.86
6	TNT	Dog	12	64	87.70	7.31
7	TNT	Dog	12	64	79.00	6.58
8	TNT	Goat	12	8	295.00	24.58
9	TNT	Goat	12	64	104.00	8.67
10	TNT	Goat	12	64	111.00	9.25
11	TNT	Goat	12	64	118.00	9.83

Figure 55. Original Bowen's test conditions.

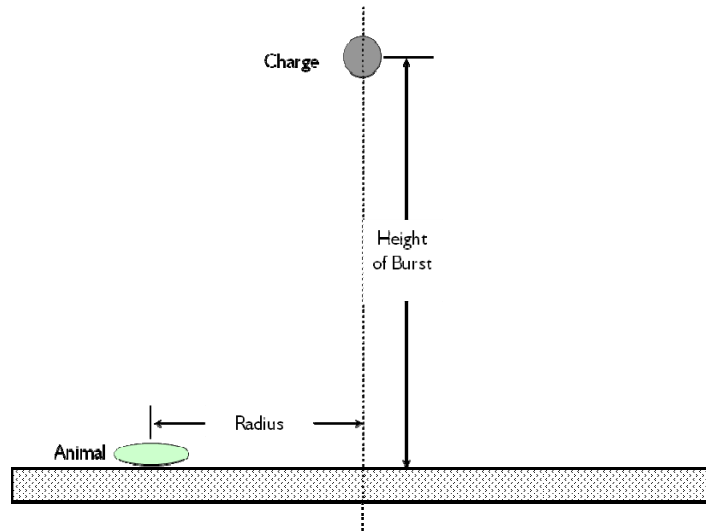


Figure 56. Bowen's test set up.

Ambient Pressure (psi)	Charge Weight (lb)	Reflected Pressure (psi)
14.7	9.8	336.88
14.7	9.8	280.53
14.7	9.8	149.45
14.7	78.4	122.50
14.7	78.4	115.52
14.7	78.4	107.43
14.7	78.4	96.78
14.7	9.8	361.38
14.7	78.4	127.40
14.7	78.4	135.98
14.7	78.4	144.55

Figure 57. Scaled Bowen's tests at sea level with same distances.

Ambient Pressure (psi)	Height of Burst (ft)	Radius (ft)	Range (ft)
14.7	6.54	1.68	6.75
14.7	7.01	1.87	7.25
14.7	7.48	2.06	7.75
	8.41	2.34	8.73
14.7	18.69	5.14	19.39
14.7	18.69	5.14	19.39
14.7	18.69	5.14	19.39
14.7	18.69	5.14	19.39
	19.63	5.37	20.35
14.7	6.54	1.68	6.75
14.7	17.76	4.91	18.42
14.7	17.76	4.91	18.42
14.7	17.76	4.91	18.42

Figure 58. Scaled Bowen's tests at sea level with same charge weights.

2.8.2 INJURY 8.3 in Simulink with Lethality Correlation

The INJURY 8.3 object codes in Simulink have been developed including the lethality correlation (Figure 59). The new object codes were converted from the INJURY 8.2 source code, and calculations were performed to verify that the new Simulink codes produce the same normalized work values as INJURY 8.2. Pressure traces from Blast Test Device (BTD) are input the same way as in INJURY 8.2. The lethality correlation for confined blast applications was derived from a subset of the BOP complex wave data that was also later validated by new test data obtained by NSRDEC in an enclosure environment using thermobaric charges.

The new INJURY 8.3 software is being packaged for release in early 2010. The Graphical User Interface (GUI) is being designed following that for TGAS. INJURY 8.3 will be integrated with TGAS as a supporting module to provide lung damage predictions, and there will also be a standalone version for users only interested in blast injury assessments. A VV&A package will be prepared and a journal paper will be written in 2010.

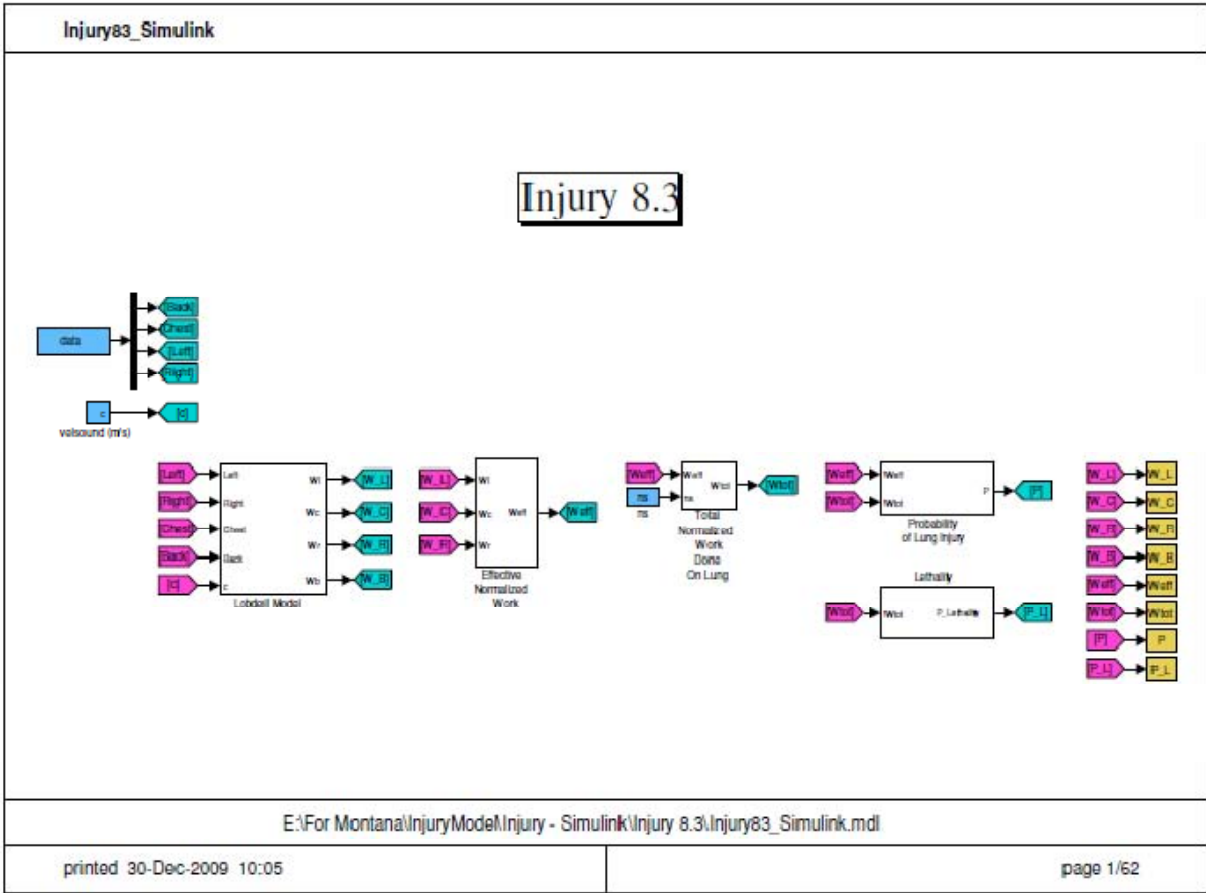


Figure 59. INJURY 8.3 in Simulink.

Product 30. INJURY 8.3 software.

3. Products

Product 1. Implemented fatigue model in Matlab for use in the Physiological-based Performance Model (PBPM).	7
Product 2. Sih, B.L., Ng, L., and Stuhmiller, J.H. “Generalization of a ‘phenomenological’ muscle fatigue model.” Technical report J0287-10-382 (in preparation).	7
Product 3. Sih, B.L., Ng, L., and Stuhmiller, J.H. “The effects of hypoxia and carboxyhemoglobin concentration on a ‘phenomenological’ model’s recovery parameter.” Technical report J0287-10-383 (in preparation).	7
Product 4. A model that predicts physiologic response to exercise.....	9
Product 5. Ng, L., Sih, B.L., and Stuhmiller, J.H. “A Model of Physiologic Response to Exercise.” Technical report J0287-10-384 (in preparation).	9
Product 6. A model that predicts physiologic response and physical performance decrement due to low oxygen and carbon monoxide exposures.....	11
Product 7. Ng, L., Sih, B.L., and Stuhmiller, J.H. “A Physiologically Based Performance Model.” Technical report J0287-10-385 (in preparation).	11
Product 8. TGAS 2.0P V&V package	12
Product 9. Crocker, G. H. (2010). "Effect of hypoxia, hyperoxia, hypercapnia and elevated carboxyhemoglobin concentration on VO ₂ max and exercise capacity in goats." University of California, Davis.....	15
Product 10. Crocker, G. H., Hayes, M. V., Weems, R. E., & Jones, J. H. 2008. "Effects of hypoxia on VO ₂ max and lactate accumulation rate in exercising goats." The American Physiological Society Intersociety Meeting: The Integrative Biology of Exercise-V. 9-24-2008.....	15
Product 11. Kwon, J., Crocker, G. H., Jones, E. M., Nye, S. M., Perloff, S. H., Hayes, M. V., Toth, B., & Jones, J. H. 2009. "Does CO Binding of Hemoglobin Affect the Ventilatory Responses to Hypoxia, Hypercapnia or Both Ventilatory Stimulants?" UC Davis School of Veterinary Medicine STARS in Science Student Research Symposium. 9-30-2009.....	15
Product 12. Matlab-based access to organized and consolidated physiological and blood chemistry parameters for steady-state and fatigue runs.....	15
Product 13. Toxic Gas Assessment Software PE v1.0	18
Product 14. A physiologic ventilatory response model integrated with the internal dose calculation for inhaled toxic gases.....	20
Product 15. Stuhmiller, J.H., Long, D. W., and Stuhmiller, L.M. (2010). Model of acute ventilation changes from inhaled gases—oxygen, carbon dioxide, and carbon monoxide (<i>in preparation</i>).....	24

Product 16. Advanced Blast Test Device (ABTD).....	27
Product 17. Rigby, P, Chan, P. (2009). “Evaluation of the Biofidelity of FMVSS No. 218 Injury Criteria,” Traffic Injury Prevention, 10:170-188.	29
Product 18. Stuhmiller, J. H. Chan, P.C., Chilton, W.E., Dang, X., Long, D.W., Rigby, P.H., Tracy, B.J., Wong, J., and Yang, W. (2009). Technical Support for Combat Helmet Sensor Fielding Project, Vol. 1: Technical, L-3 Communications/Jaycor, San Diego, CA. Midterm Report J0287-09-366, 108 pp., Jan. 2009.....	38
Product 19. Stuhmiller, J. H. Chan, P.C., Chilton, W.E., Dang, X., Long, D.W., Rigby, P.H., Tracy, B.J., Wong, J., and Yang, W. (2009). Technical Support for Combat Helmet Sensor Fielding Project, Vol. 1: Appendices, L-3 Communications/Jaycor, San Diego, CA. Midterm Report J0287-09-366A, 110 pp., Jan. 2009.....	38
Product 20. Stuhmiller, J. H. Chan, P.C., Chilton, W.E., Dang, X., Long, D.W., Rigby, P.H., Tracy, B.J., Wong, J., and Yang, W. (2009). Technical Support for Combat Helmet Sensor Fielding Project, Vol. 1: Technical, L-3 Communications/Jaycor, San Diego, CA. Annual Report J0287-09-376, 110 pp., Aug. 2009.	38
Product 21. Stuhmiller, J. H. Chan, P.C., Chilton, W.E., Dang, X., Long, D.W., Rigby, P.H., Tracy, B.J., Wong, J., and Yang, W. (2009). Technical Support for Combat Helmet Sensor Fielding Project, Vol. 1: Appendices, L-3 Communications/Jaycor, San Diego, CA. Annual Report J0287-09-376, 138 pp., Aug. 2009.	38
Product 22. P. Chan, MacFadden, L., Dang, X., Ho, K., Maffeo, M., Carboni, M., and DeCristofano, B. (2010). “Study of Material Effects on Blast Lung Injury using Normalized Work Method,” accepted for presentation at PASS2010, Quebec, Canada, September 2010.	40
Product 23. INJURY-A – A model for predicting blast injury with armor effects.	40
Product 24. Whang, C., Ho, K., Long, D., and Chan, P. (2009) “MBTD Data Analysis Algorithm and Software,” Technical Report J0287-09-368 for Contract W81XWH-06-C-0051, CLIN0002” prepared for NSRDEC.....	42
Product 25. MBTD data screening software.....	42
Product 26. Sheep Blast Test Device (SBTD).....	43
Product 27. Human Thoracic Model.....	47
Product 28. Blast Trauma Assessment Tool (BTAT) software.	47
Product 29. Martin, P., Craig, M., Ridella, S., Rigby, P., and Chan, P. (2009) “OOP Air Bag Tests using the 5 th Percentile Female THOR and Hybrid III Dummies,” Paper Number 09-0546, 21 st International Technical Conference on the Enhanced Safety of Vehicles Conference (ESV), Stuttgart, Germany, June 15-18, 2009.	49
Product 30. INJURY 8.3 software.	52

4. References

- Boggs, D. F. (1991). Comparative control of respiration. Comparative Biology of the Normal Lung. R. A. Parent (ed.). Boca Raton, FL, CRC Press: 309-350.
- Chang, H. K. and M. Paiva (1898). Respiratory Physiology, An Analytical Approach. New York, Marcel Dekker.
- Chiari, L., G. Avanzolini and M. Ursino (1997). "A comprehensive simulator of the human respiratory system: validation with experimental and simulated data." *Ann Biomed Eng* **25**(6): 985-99.
- Dempsey, J. A. and A. I. Pack (1994). Regulation of Breathing. New York, Marcel Dekker, Inc.
- Ding, J., A. S. Wexler and S. A. Binder-Macleod (2000). "A predictive model of fatigue in human skeletal muscles." *Journal of Applied Physiology* **89**(4): 1322.
- Doblar, D. D., T. V. Santiago and N. H. Edelman (1977). "Correlation between ventilatory and cerebrovascular responses to inhalation of CO." *J Appl Physiol* **43**(3): 455-62.
- Duffin, J. (1989). The effect of exercise on the central and peripheral chemoreceptor thresholds to carbon dioxide in man. Respiratory Control, A Modeling Perspective. G. D. Swanson, F. S. Grodins and R. L. Hughson (ed.). New York, Plenum Press: 63-70.
- Duffin, J. (1991). "A model of respiratory rhythm generation." *Neuroreport* **2**(10): 623-6.
- Duffin, J. (1994). "Neural drives to breathing during exercise." *Can J Appl Physiol* **19**(3): 289-304.
- Duffin, J. and G. V. McAvoy (1988). "The peripheral-chemoreceptor threshold to carbon dioxide in man." *J Physiol (Lond)* **406**: 15-26.
- Duffin, J., R. M. Mohan, P. Vasiliou, R. Stephenson and S. Mahamed (2000). "A model of the chemoreflex control of breathing in humans: model parameters measurement." *Respir Physiol* **120**(1): 13-26.
- Fidone, S. J. and C. Gonzales (1986). Initiation and control of chemoreceptor activity in the carotid body. Section 3: The Respiratory System. A. P. Fishman (ed.). Bethesda, MD, American Physiology Society. **2**: 247-312.
- Fitzgerald, R. S. and S. Lahiri (1986). IReflex responses to chemoreceptor stimulation. Section 3: The Respiratory System. A. P. Fishman (ed.). Bethesda, MD, American Physiology Society. **2**: 247-312.
- Giat, Y., J. Mizrahi and M. Levy (1993). "A musculotendon model of the fatigue profiles of paralyzed quadriceps muscle under FES." *IEEE Trans Biomed Eng* **40**(7): 664-74.
- Grodins, F. S. (1964). "Regulation of pulmonary ventilation." *Physiologist* **7**: 319-333.
- Grodins, F. S., J. Buell and A. J. Bart (1967). "Mathematical analysis and digital simulation of the respiratory control system." *J Appl Physiol* **22**(2): 260-76.
- Grodins, F. S. and S. M. Yamashiro (1973). "Optimization of the mammalian respiratory gas transport system." *Annu Rev Biophys Bioeng* **2**: 115-30.

- Gu, Z. and A. J. Januszkiewicz (2002). "Effects of brief exposure to very high concentration of nitrogen dioxide on respiratory function in awake rats." *AAAS Proceedings*: A96.
- Gu, Z., A. J. Januszkiewicz and M. A. Mayorga (2002). "Consequences of brief exposure to high-concentration carbon monoxide in awake rats." *Toxicologist* **60**: 1689.
- Gu, Z., A. J. Januszkiewicz, M. A. Mayorga, G. D. Coleman and C. R. Morrisette (2005). "Consequences of brief exposure to high concentrations of carbon monoxide in conscious rats." *Inhal Toxicol* **17**(13): 755-64.
- Gu, Z., A. J. Januszkiewicz, C. D. McKinley, M. A. Mayorga, L. M. Stuhmiller and J. H. Stuhmiller (2000). "Biochemical and respiratory changes caused by brief exposure to high concentration carbon monoxide and carbon dioxide in awake rats." *The Toxicologist* **54**(1): 19.
- Hlastala, M. P. and A. J. Berger (2001). Physiology of Respiration. New York, Oxford Press.
- Honda, Y., H. Miyamoto, K. Konno and J. Widdicombe (1992). Control of Breathing and Its Modeling Perspective. New York, Plenum Press.
- Levy, M., J. Mizrahi and Z. Susak (1990). "Recruitment, force and fatigue characteristics of quadriceps muscles of paraplegics isometrically activated by surface functional electrical stimulation." *J Biomed Eng* **12**(2): 150-6.
- Longobardo, G., C. Evangelisti, N. Prabhakar and N. S. Cherniack (2001). "Neural drives and breathing stability." *Adv Exp Med Biol* **499**: 453-8.
- Longobardo, G., C. J. Evangelisti and N. S. Cherniack (2003). "Effects of controller dynamics on simulations of irregular and periodic breathing." *Adv Exp Med Biol* **536**: 389-99.
- Longobardo, G. S., N. S. Cherniack and A. Damokosh-Giordano (1980). "Possible optimization of respiratory controller sensitivity." *Ann Biomed Eng* **8**(2): 143-58.
- Longobardo, G. S., B. Gothe, M. D. Goldman and N. S. Cherniack (1982). "Sleep apnea considered as a control system instability." *Respir Physiol* **50**(3): 311-33.
- Mateika, J. H. and J. Duffin (1992). "Changes in ventilation at the start and end of moderate and heavy exercise of short and long duration." *European Journal of Applied Physiology* **65**: 234-40.
- Stuhmiller, J. H. and L. M. Stuhmiller (2005). "A mathematical model of ventilation response to inhaled carbon monoxide." *J Appl Physiol* **98**(6): 2033-44.
- Swanson, G. D., F. S. Grodins and R. L. Hughson (1998). Respiratory Control, A Modeling Perspective. New York, Plenum Press.
- Ursino, M. and E. Magosso (2004). "Interaction among humoral and neurogenic mechanisms in ventilation control during exercise." *Ann Biomed Eng* **32**(9): 1286-99.
- Ursino, M., E. Magosso and G. Avanzolini (2001). "An integrated model of the human ventilatory control system: the response to hypercapnia." *Clin Physiol* **21**(4): 447-64.
- Ursino, M., E. Magosso and G. Avanzolini (2001). "An integrated model of the human ventilatory control system: the response to hypoxia." *Clin Physiol* **21**(4): 465-77.

- Wagner, P. D., G. E. Gale, R. E. Moon, J. R. Torre-Bueno, B. W. Stolp and Saltzman (1986). "Pulmonary gas exchange in humans exercising at sea level and simulated altitude." *J. Appl. Physiol.* **61**(1): 260-270.
- Weyand, P. G., C. S. Lee, R. Martinez-Ruiz, M. W. Bundle, M. J. Bellizzi and S. Wright (1999). "High-speed running performance is largely unaffected by hypoxic reductions in aerobic power." *J Appl Physiol* **86**(6): 2059-64.
- Whipp, B. J. (1987). The Control of Breathing in Man. Philadelphia, PA, University of Pennsylvania Press.